(12) INTERNATIONAL APPLICATION PUBLISHED UNDER THE PATENT COOPERATION TREATY (PCT)

(19) World Intellectual Property Organization
International Bureau

(43) International Publication Date
26 May 2017 (26.05.2017)

WIPO | PCT

(10) International Publication Number
WO 2017/087403 A1

(51) International Patent Classification:
H01M 4/131 (2010.01) *H01M 4/525* (2010.01)
H01M 4/48 (2010.01) *H01M 10/0525* (2010.01)
H01M 4/505 (2010.01)

(21) International Application Number:
PCT/US2016/062067

(22) International Filing Date:
15 November 2016 (15.11.2016)

(25) Filing Language: English

(26) Publication Language: English

(30) Priority Data:
62/255,676 16 November 2015 (16.11.2015) US
62/343,469 31 May 2016 (31.05.2016) US

(71) Applicant: **THE REGENTS OF THE UNIVERSITY OF CALIFORNIA** [US/US]; 1111 North Franklin Street, 5th Floor, Oakland, California 94607 (US).

(72) Inventors: **MENG, Ying Shirley**; 1661 Beryl Street, San Diego, California 92109 (US). **ZHANG, Minghao**; 9450 Gilman Drive #40090, La Jolla, California 92092 (US). **LIU, Haodong**; 4043 H, Miramar Street, La Jolla, California 92037 (US). **QIAN, Danna**; 9500 Gilman Drive, MC 0910, La Jolla, California 92093 (US). **FANG, Chengcheng**; 9500 Gilman Drive, MC 0910, La Jolla, California 92093 (US).

(74) Agent: **FALLON, Steven P.**; Greer, Burns & Crain, Ltd., 300 South Wacker Drive, Suite 2500, Chicago, Illinois 60606 (US).

(81) Designated States *(unless otherwise indicated, for every kind of national protection available)*: AE, AG, AL, AM, AO, AT, AU, AZ, BA, BB, BG, BH, BN, BR, BW, BY, BZ, CA, CH, CL, CN, CO, CR, CU, CZ, DE, DJ, DK, DM, DO, DZ, EC, EE, EG, ES, FI, GB, GD, GE, GH, GM, GT, HN, HR, HU, ID, IL, IN, IR, IS, JP, KE, KG, KN, KP, KR, KW, KZ, LA, LC, LK, LR, LS, LU, LY, MA, MD, ME, MG, MK, MN, MW, MX, MY, MZ, NA, NG, NI, NO, NZ, OM, PA, PE, PG, PH, PL, PT, QA, RO, RS, RU, RW, SA, SC, SD, SE, SG, SK, SL, SM, ST, SV, SY, TH, TJ, TM, TN, TR, TT, TZ, UA, UG, US, UZ, VC, VN, ZA, ZM, ZW.

(84) Designated States *(unless otherwise indicated, for every kind of regional protection available)*: ARIPO (BW, GH, GM, KE, LR, LS, MW, MZ, NA, RW, SD, SL, ST, SZ, TZ, UG, ZM, ZW), Eurasian (AM, AZ, BY, KG, KZ, RU, TJ, TM), European (AL, AT, BE, BG, CH, CY, CZ, DE, DK, EE, ES, FI, FR, GB, GR, HR, HU, IE, IS, IT, LT, LU, LV, MC, MK, MT, NL, NO, PL, PT, RO, RS, SE, SI, SK,

[Continued on next page]

(54) Title: LITHIUM-EXCESS CATHODE MATERIAL AND CO-PRECIPITATION FORMATION METHOD

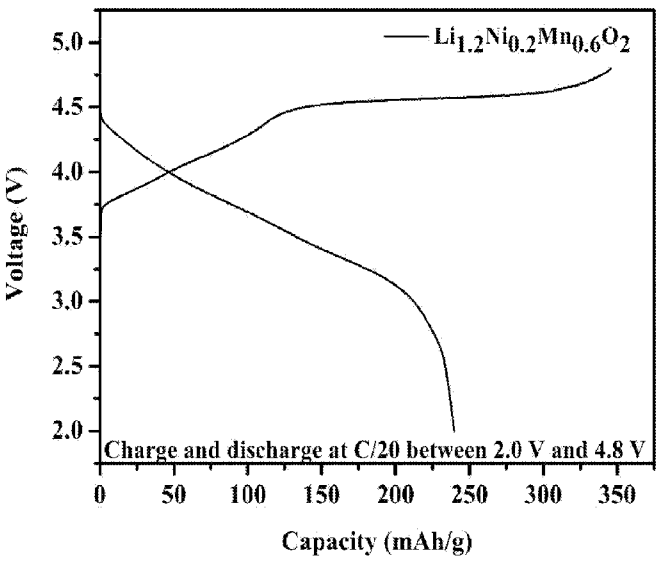

FIG. 3

(57) Abstract: A lithium-excess cathode material according to Li1+xNiaMnbCocModO2-y ($0<x<0.3$, $0\leq a\leq 1$, $0\leq b\leq 1$, $0\leq c\leq 1$, $0\leq d\leq 0.2$, $0\leq y\leq 0.25$) in the form of secondary spherical microparticles formed from primary spherical nanoparticles. The primary nanoparticles can be in the range of ~130nm to 170nm and the secondary in the range of ~2-3 μm. A method of formation includes mixing a carbonates or hydroxides solution into a mixed solution of transition metal (M) ions with predetermined stoichiometry under stirring, and aging resulting transition metal carbonates or hydroxides at a predetermined temperature for period of time to produce primary nanoparticles of a predetermined size. A gas-solid interface reaction to uniformly creating oxygen vacancies without affecting structural integrity of Li-excess layered oxides is also provided.

WO 2017/087403 A1

SM, TR), OAPI (BF, BJ, CF, CG, CI, CM, GA, GN, GQ, GW, KM, ML, MR, NE, SN, TD, TG).

Published:

— *with international search report (Art. 21(3))*

LITHIUM-EXCESS CATHODE MATERIAL AND CO-PRECIPITATION FORMATION METHOD

STATEMENT OF GOVERNMENT INTEREST

[001] This invention was made with government support under grant no. DE-AC02-05CH11231 (subcontract no 7056412) awarded by the Department of Energy. The government has certain rights in the invention.

PRIORITY CLAIM AND REFERENCE TO RELATED APPLICATION

[002] The application claims priority under 35 U.S.C. §119 and all applicable statutes and treaties from prior United States provisional application serial number 62/080,718, which was filed November 17, 2015, and from prior United States provisional application serial number 62/343,469, which was filed May 31, 2016.

FIELD

[003] A field of the invention is lithium ion batteries. The invention particularly concerns lithium-excess cathode materials and cathodes. Lithium batteries with cathodes of the invention have widespread application, from a variety of mobile device power applications to hybrid and electrically powered vehicles. The invention particularly

relates to non-aqueous rechargeable lithium and lithium ion electrochemical cells and batteries. Such cells can operate at ambient temperature. These rechargeable lithium and lithium ion cells and batteries may be used for many energy storage applications, including large-scale stationary electrical storage for the electrical grid. Other applications for lithium ion batteries include, but are not limited to portable device, transportation, defense products, and aerospace products.

BACKGROUND

[004] Cathode materials with micrometer-sized spherical particles composed of nanoparticles are known to exhibit excellent electrochemical properties. Lithium transition metal layered oxide spherical particles can be prepared through a hydroxide or a carbonate co-precipitation process.

[005] S.H Park et. al reported that $Li_{1+x}(Ni_{1/3}Co_{1/3}Mn_{1/3})_{1-x}O_2$ cathode materials synthesized by a conventional co-precipitation method using a continuously stirred tank reactor can improve both physical and electrochemical performance to a large extent. "Physical and electrochemical properties of spherical $Li_{1+x}(Ni_{1/3}Co_{1/3}Mn_{1/3})_{1-x}O_2$ cathode materials," Journal of Power Sources, 177 (2008) 177-183. The publication reported a uniform, spherical morphology via a coprecipitation using a continuously stirred tank reactor method. The publication also reported a second synthesis route that involved the use of an M_3O_4 ($M = Ni_{1/3}Co_{1/3}Mn_{1/3}$) spinel compound, obtained from the carbonate $(Ni_{1/3}Co_{1/3}Mn_{1/3})CO_3$ precursor. The publication states that both $Li_{1+x}(Ni_{1/3}Co_{1/3}Mn_{1/3})_{1-x}O_2$ products were highly uniform, having a narrow particle size distribution (10-μm average particle size). This is

attributed to the homogeneity and spherical morphology of the starting mixed-metal carbonate precursor.

[006] A. Bommel et.al reported upon a growth mechanism of co-precipitated spherical and dense nickel, manganese, and cobalt-containing hydroxides, and the influence of aqueous ammonia on the co-precipitation reaction. "Analysis of the Growth Mechanism of Coprecipitated Spherical and Dense Nickel, Manganese, and Cobalt-Containing Hydroxides in the Presence of Aqueous Ammonia," Chemistry of Materials, 21 (2009) 1500-1503. The publication identifies the roles of pH, transition-metal type(s), and aqueous ammonia concentration as being most important in the synthesis of dense materials. Different pH ranges were identified for different metal hydroxides of $Ni(OH)_2$, $Ni_{1/2}Mn_{1/2}(OH)_2$, and $Ni_{1/3}Mn_{1/3}Co_{1/3}(OH)_2$. The publication attributed metal hydroxide particle growth to a dissolution–recrystallization type mechanism during synthesis.

[007] D. Wang et.al reported upon a growth mechanism of co-precipitated spherical carbonate precursor for high capacity Li-ion battery cathodes and the pH zone that favors carbonate co-precipitation reaction. "Growth mechanism of $Ni_{0.3}Mn_{0.7}CO_3$ precursor for high capacity Li-ion battery cathodes," Journal of Materials Chemistry, 21 (2011) 9290-9295. The publication reported that Transition metal carbonate ($Ni_{0.3}Mn_{0.7}CO_3$) was co-precipitated as the precursor for Li- and Mn-enriched composite materials. An optimal pH range was reportedly determined based upon chemical equilibriums between the products and reactants. The publication reported that early stages of co-precipitation produced a nonhomogeneous particle size distribution and a nonhomogeneous chemical composition. The publication reported that about five hours were required for the co-precipitation to produce homogenous particle size and distribution, albeit with particle sizes greater than 30 μm.

[008] The above publications are illustrative of co-precipitation methods for production of lithium transition metal layered oxide spherical particles that can be prepared through a hydroxide or a carbonate co-precipitation process. Generally, these traditional co-precipitation methods require delicate control of the concentration of precursors and ammonium hydroxide to obtain homogenous spherical precursors, and many only produce 20 or 30 μm or larger sized particles. The large particle size, however, may introduce several kinetic limitations during initial activation. In addition, such large size particles can crack during an initial charging process or during discharge/recharge, leading to capacity and voltage degradation over extended cycling. See, e.g., Chen et al., "Study on the synthesis–microstructure-performance relationship of layered Li-excess nickel–manganese oxide as a Li-ion battery cathode prepared by high-temperature calcination," Journal of Materials Chemistry A, 1 (2013) 10847-10856. The publication reported that internal cracks within these large size particles form even before any electrochemical cycling, which causes cycling degradation and might be a common problem encountered in the conventional precipitation–calcination process.

[009] Additionally, in Li-ion cathode materials, oxygen vacancies have been investigated as potentially playing a role in determining the material's electron and ion transport properties. See, e.g., Armstrong, A. R. *et al.* "Demonstrating oxygen loss and associated structural reorganization in the lithium battery cathode $Li[Ni_{0.2}Li_{0.2}Mn_{0.6}]O_2$" J. Am. Chem. Soc. 128, 8694-8698 (2006); Koga, H. *et al.*, "Different oxygen redox participation for bulk and surface: A possible global explanation for the cycling mechanism of $Li_{1.20}Mn_{0.54}Co_{0.13}Ni_{0.13}O_2$", J. Power Sources, 236, 250-258 (2013). However, the introduction of high levels of oxygen vacancies by prior techniques is known to harm bulk material properties and provide less than high quality bulk material. Previous

work by the inventors and collaborators has shown that oxygen vacancies generated during the high-potential electrochemical process can facilitate the migration and surface structural transformation of transition metals, finally leading to their potential degradation during extended cycles. Xu, B., Fell, C. R., Chi, M. & Meng, Y. S., "Identifying surface structural changes in layered Li-excess nickel manganese oxides in high voltage lithium ion batteries: A joint experimental and theoretical study," Energy Environ. Sci. 4, 2223-2233 (2011); Fell, C. R. *et al.*, "Correlation between oxygen vacancy, microstrain, and cation distribution in lithium-excess layered oxides during the first electrochemical cycle," Chem. Mater. 25, 1621-1629 (2013); Qian, D., Xu, B., Chi, M. & Meng, Y. S., "Uncovering the roles of oxygen vacancies in cation migration in lithium excess layered oxides," Phys. Chem. Chem. Phys. 16, 14665-14668 (2014). Previous publications have described creation of oxygen vacancies with a reducing atmosphere. Kubota, K. *et al.*, "Direct synthesis of oxygen-deficient Li_2MnO_{3-x} for high capacity lithium battery electrodes," Journal of Power Sources 216, 249-255 (2012). Other publications report use of leaching with acid accompanied by heat treatment. Kang, S. H., Johnson, C. S., Vaughey, J. T., Amine, K. & Thackeray, M. M., "The effects of acid treatment on the electrochemical properties of $0.5Li_2MnO_3$-$0.5LiNi_{0.44}Co_{0.25}Mn_{0.31}O_2$ electrodes in lithium cells,". J. Electrochem. Soc. 153, A1186-A1192 (2006). Bulk structures reported in our previous works and from other techniques to produce oxygen vacancies easily transforms from a pure layered phase to spinel- and/or rock-salt phases that immensely damages the rate capability and cycling stability.

SUMMARY OF THE INVENTION

[0010] An embodiment of the invention is a lithium-excess cathode material according to $Li_{1+x}Ni_aMn_bCo_cMo_dO_{2-y}$ ($0<x<0.3$, $0\leq a\leq 1$, $0\leq b\leq 1$, $0\leq c\leq 1$, $0\leq d\leq 0.2$, $0\leq y\leq 0.25$) in the form of secondary spherical microparticles formed from primary spherical nanoparticles. The primary nanoparticles can be in the range of ~130nm to 170nm and the secondary in the range of ~2–3 μm. A method of formation includes mixing a carbonates or hydroxides solution into a mixed solution of transition metal (M) ions with predetermined stoichiometry under stirring, and aging resulting transition metal carbonates or hydroxides at a predetermined temperature for period of time to produce primary nanoparticles of a predetermined size.

[0011] Particular preferred materials include $Li_{1.2}Ni_{0.2}Mn_{0.6}O_2$, $Li_{1.2}Ni_{0.136}Mn_{0.544}Co_{0.136}O_2$, $Li_{1.1}Ni_{0.2}Mn_{0.6}O_{1.95}$, $Li_{1.13}Ni_{0.3}Mn_{0.57}O_2$, $Li_{1.144}Ni_{0.136}Co_{0.136}Mn_{0.544}O_{1.92}$, and $Li_{1.18}Ni_{0.135}Co_{0.135}Mn_{0.539}Mo_{0.01}O_2$. Preferree mateirals can also include a lithium lanthanum titanium oxide coating. Preferred methods can introduce and preferred materials can include excess oxygen vacancies.

BRIEF DESCRIPTION OF DRAWINGS

[0012] FIG. 1 is an XRD pattern of a sample $Li_{1.2}Ni_{0.2}Mn_{0.6}O_2$ synthesized by a preferred co-precipitation method of the invention;

[0013] FIGs. 2A-2B are SEM images at different magnifications of sample $Li_{1.2}Ni_{0.2}Mn_{0.6}O_2$: synthesized by a preferred co-precipitation method of the invention and FIGs. 2C-2D of $Li_{1.2}Ni_{0.2}Mn_{0.6}O_2$: synthesized by conventional co-precipitation method without morphology control;

[0014] FIG. 3 is an initial charge/discharge plot of $Li_{1.2}Ni_{0.2}Mn_{0.6}O_2$ synthesized by a preferred co-precipitation method of the invention;

[0015] FIGs. 4A and 4B are plots of cycling performance of sample $Li_{1.2}Ni_{0.2}Mn_{0.6}O_2$: synthesized by a preferred co-precipitation method of the invention and FIGs. 4C and 4D of $Li_{1.2}Ni_{0.2}Mn_{0.6}O_2$: synthesized by conventional co-precipitation method without morphology control;

[0016] FIGs. 5A-5C are respectively an XRD pattern and SEM images of different magnifications of sample $Li_{1.2}Ni_{0.136}Mn_{0.544}Co_{0.136}O_2$ synthesized by a preferred co-precipitation method of the invention;

[0017] FIG. 6 is an initial charge/discharge plot of $Li_{1.2}Ni_{0.136}Mn_{0.544}Co_{0.136}O_2$ synthesized by a preferred co-precipitation method of the invention;

[0018] FIGs. 7A-7C are respectively an XRD pattern and SEM images of different magnifications of sample $Li_{1.1}Ni_{0.2}Mn_{0.6}O_{1.95}$ synthesized by a preferred co-precipitation method of the invention;

[0019] FIG. 8A is an XRD pattern and FIGs. 8B-8D plots of electrochemical performance of morphology controlled $Li_{1.13}Ni_{0.3}Mn_{0.57}O_2$ synthesized by a preferred co-precipitation method of the invention and coated with Lithium Lanthanum Titanium Oxides (LLTO) under different coating conditions;

[0020] FIG. 9 is a time of flight neutron diffraction (ND) pattern of sample $Li_{1.144}Ni_{0.136}Co_{0.136}Mn_{0.544}O_{1.92}$ synthesized by a preferred co-precipitation method of the invention;

[0021] FIG. 10 is a first charge-discharge profile of sample $Li_{1.144}Ni_{0.136}Co_{0.136}Mn_{0.544}O_{1.92}$ synthesized by a preferred co-precipitation method of the invention;

[0022] FIG. 11 is a first charge-discharge profile and cycling performance of sample $Li_{1.18}Ni_{0.135}Co_{0.135}Mn_{0.539}Mo_{0.01}O_2$ synthesized by a preferred co-precipitation method of the invention;

[0023] FIGs. 12A and 12B are time of flight neutron diffraction patterns illustrating that a preferred gas solid interfacial modification method to create oxygen vacancies in lithium excess materials has little effect upon crystal structures and bulk electronic properties;

[0024] FIG. 13A is a charge-discharge characteristics that compare preferred lithium excess materials with and without excess oxygen vacancies and FIG. 13B compares differential capacities.

DETAILED DESCRIPTION OF THE PREFERRED EMBODIMENTS

[0025] Preferred embodiments provide lithium-excess cathode materials and co-precipitation fabrication methods. Preferred cathode materials are morphology-controlled lithium-excess materials $Li_{1+x}Ni_aMn_bCo_cMo_dO_{2-y}$ ($0<x<0.3$, $0\leq a\leq 1$, $0\leq b\leq 1$, $0\leq c\leq 1$, $0\leq d\leq 0.2$, $0\leq y\leq 0.25$) with or without oxygen vacancies. The cathode materials are well-suited for use as lower-cost, high energy density cathodes for lithium ion batteries. Present materials have potential to increase the overall energy density of state-of-the-art lithium ion batteries by 20-25%. Preferred co-precipitation methods do not require aqueous ammonia addition during the formation process. Preferred methods provide lithium-excess material with uniform spherical morphology. Morphology-controlled lithium-excess material of the invention shows improved cycling ability and minimized voltage degradation compared to prior comparable materials known to the inventors. No cracking of the materials was observed.

[0026] Preferred embodiments further provide advantageous oxygen vacancies without affecting bulk properties. Preferred fabrication methods provide Li-ion cathode materials with stoichiometries characterized by oxygen vacancies that lead to improved electron and ion transport properties. Electron energy loss spectroscopy (EELS) mapping reveals oxygen vacancies have been successfully introduced on the 0-20 nm of the surface without a noticeable interruption in the bulk-structure. Electrochemical measurements prove that surface oxygen vacancies introduction in Li excess cathodes without severe structural destruction has a considerable effect on improving electrochemical performance.

[0027] A preferred co-precipitation method includes: An appropriate amount of carbonates or hydroxides was dissolved in deionized water to produce the

desired particular compound in accordance with molar ratios to achieve that compound, and then added into a mixed solution of transition metal (M) ions with appropriate stoichiometry under stirring. An appropriate amount can be determined by the transition metal solution concentration. An equal concentration for carbonates and double concentration for hydroxides compared with transition metal concentration is used in preferred embodiments. The resulting transition metal carbonates or hydroxides was transferred to Teflon lined stainless steel autoclave, and then aged at selected temperature (ranging from 40 °C to 80 °C) for suitable period of time (e.g. 2 to 20 hours). Thereafter, the resulting powder was washed, dried and then mixed with a stoichiometric amount of lithium carbonate or lithium hydroxide, followed by calcination at selected temperature (ranging from 400 °C to 1000 °C) for suitable period of time (e.g. 6 to 40 hours).

[0028] The obtained sample is phase pure lithium-excess material (which can be indexed as a hexagonal α-$NaFeO_2$ structure) confirmed by XRD spectrum. Sharp reflections in the XRD patterns reveal the high crystallinity of the sample. The obtained material has spherical morphology with excellent dispersion. The secondary particles are dense, and have an average diameter of approximately 2-3 μm. These secondary spherical particles consist of primary particles with particle size of ~130nm to 170nm and preferably approximately 150 nm.

[0029] When charged and discharged at a rate of 0.05 C between 2.0 V and 4.8 V, one sample of this invention can deliver a discharge capacity of about 250 mA h g^{-1}. Compared with the sample without morphology control, the morphology control sample not only shows a large discharge capacity at the first cycle, but also it exhibits almost the same capacity and voltage curve at the 80th cycle, which shows the preferred co-precipitation method may be promising for resolving the problem of the capacity and voltage fading during cycling of lithium-excess materials.

[0030] Since preferred cathodes are rich in manganese, they are expected to be low in cost compared to similar lithium metal oxide compounds, and exhibit high power, high energy, and long cycle life times.

[0031] In a preferred embodiment, $Li_{1.2}Ni_{0.2}Mn_{0.6}O_2$ (0.5 $LiNi_{0.5}Mn_{0.5}O_2$•0.5 Li_2MnO_3) is first obtained due to its high reversible discharge capacity (250 mAh g^{-1}) as well as relatively lower price (compare to Co containing materials). To make uniform spherical $Li_{1.2}Ni_{0.2}Mn_{0.6}O_2$ sample, precursor particles $(Ni_{0.25}Mn_{0.75})CO_3$ with homogenous composition were first synthesized via a preferred co-precipitation method.

[0032] In a preferred method, an appropriate molar amount of Li_2CO_3 (the molar ratio of carbonate ions to transitional metal ions is preferably 1:1, and within 1.05:1 to 1:1) was dissolved in 60 mL deionized water, and then added dropwise into 10 ml of a mixed solution of $Ni(NO_3)_2$ and $Mn(NO_3)_2$ (Ni:Mn = 1:3 in molar ratio) under stirring. The resulting slurry was transferred to 100 mL Teflon lined stainless steel autoclave, and then aged at 80 °C for 12 h, the resulting $(Ni_{0.25}Mn_{0.75})CO_3$ precursor was washed several times by pure water to remove residual Li^+, and dried in a vacuum oven at 80 °C over night. For secondary particles of a predetermined 2-3 micrometer size , the aging should be conducted at 70 to 80°C for 10h to 15h. For an arbitrary smaller predetermined size, the aging can be conducted from 40 to 80C for 2h to 20h. Thereafter, the $(Ni_{0.25}Mn_{0.75})CO_3$ powder was mixed with a stoichiometric amount of Li_2CO_3, and was calcined at ~400-500 °C, most preferably ~500°C for ~3-7 h, most preferably ~5 h, in a 50 ml porcelain crucible, and then heated up to ~750-1000, most preferably ~900 °C and kept at this temperature for ~3-20h, most preferably ~6 h followed by quenching in the air. This serves to calciante the powders to form a pure phase.

[0033] Experiments have obtained example materials with spherical morphology with micro-particle (secondary particle) sizes in the range of 2–3 μm are

producd with the preferred calcination times and temperatures and with the aging process. These micro-spherical secondary particles are composed of a plurality of primary particles with diameters of about 150 nm on average, and are more generally ~130nm to 170nm.

[0034] A preferred embodiment provides a morphology controlled lithium excess material $Li_{1+x}Ni_aMn_bCo_cMo_dO_{2-y}$ ($0<x<0.3$, $0\leq a\leq 1$, $0\leq b\leq 1$, $0\leq c\leq 1$, $0\leq d\leq 0.2$, $0\leq y\leq 0.25$) as high energy density cathode for lithium ion batteries. This preferred lithium excess material with morphology control can be synthesized through a preferred co-precipitation method without any aqueous ammonia addition. The preferred material has spherical morphology with an average diameter of approximately ~3 μm. These secondary spherical particles consist of primary particles with particle size approximately 150 nm. The morphology controlled material can minimize voltage decay problem as well as improve capacity retention during cycling. The implementation of Li-excess materials in this invention as the cathode material in lithium ion batteries can increase the overall energy density of the state-of-the-art lithium ion batteries by 20-25%.

[0035] A preferred embodiment electrode is formed from an active material of composition $Li_{1.2}Ni_{0.2}Mn_{0.6}O_2$ ($0.5\ LiNi_{0.5}Mn_{0.5}O_2 \bullet 0.5\ Li_2MnO_3$). In a preferred formation method, precursor particles $(Ni_{0.25}Mn_{0.75})CO_3$ with homogenous composition were first synthesized via a preferred co-precipitation method and aged to achieve the preferred secondary particle size. Thereafter, the $(Ni_{0.25}Mn_{0.75})CO_3$ powder was mixed with a stoichiometric amount of Li_2CO_3, and was calcined at 500 °C for 5 h in a 50 ml porcelain crucible, and then heated up to 900 °C and kept at this temperature for 6 h followed by quenching in the air. XRD has been used to confirm the obtained spherical sample is phase pure lithium-excess material. SEM images show the obtained precursor has spherical morphology with particle sizes in the range of 2–3 μm. These micro-

spherical particles are composed of primary particles with diameters of about 150 nm on average. We have studied the effects of morphology control process on the electrochemical performance of $Li_{1.2}Ni_{0.2}Mn_{0.6}O_2$ cathode materials. When charged and discharged at a rate of 0.05 C between 2.0 V and 4.8 V, the sample can deliver a discharge capacity of about 250 mA h g^{-1}. Compared with the sample without morphology control, the morphology control sample not only shows a large discharge capacity at the first cycle, but also it exhibits almost the same capacity and voltage curve at the 80th cycle, which shows the preferred co-precipitation method may be promising for resolving the problem of the capacity and voltage fading during cycling of lithium-excess materials.

[0036] Morphology controlled lithium excess material $Li_{1+x}Ni_aMn_bCo_cMo_dO_{2-y}$ ($0<x<0.3$, $0\leq a\leq 1$, $0\leq b\leq 1$, $0\leq c\leq 1$, $0\leq d\leq 0.2$, $0\leq y\leq 0.25$) are provided as high energy density cathode for lithium ion batteries. This lithium excess material with morphology control is synthesized through a preferred co-precipitation method without any aqueous ammonia concentration control during the process, i.e., no aqueous ammonia needs to be added during the process.

[0037] In another preferred embodiment, $Li_{1.2}Ni_{0.136}Mn_{0.544}Co_{0.136}O_2$ is obtained following the synthesis protocol above. The difference is the molar ratios chosen, e.g., Ni:Mn:Co = 1:4:1 in molar ratio in the precursor solution. Sharp reflections in the XRD patterns reveal the high crystallinity of the samples. SEM images for the $Li_{1.2}Ni_{0.136}Mn_{0.544}Co_{0.136}O_2$ powder synthesized by the preferred co-precipitation show the size of the primary particles increases to 200 nm due to the lithiation reaction and crystal growth, and the spherical morphology of the precursor is preserved at high temperature. Moreover, we note that the agglomeration of the grains for $Li_{1.2}Ni_{0.136}Mn_{0.544}Co_{0.136}O_2$ powder synthesized by our preferred method is controlled by aging in the sealed container, the time of which determines

the size of the secondary particles that are formed and brings an improvement of the physical properties of the material. The sample $Li_{1.2}Ni_{0.136}Mn_{0.544}Co_{0.136}O_2$synthesized by co-precipitation method shows a high discharge capacity (270 mAh/g) at 0.1 C rate and small irreversible capacity for the first cycle.

[0038] In another preferred embodiment, $Li_{1.1}Ni_{0.2}Mn_{0.6}O_{1.95}$ is obtained following the synthesis protocol described above with appropriate molar ratios of precursors. Sharp reflections in measured XRD patterns reveal the high crystallinity of the samples. SEM images for the $Li_{1.1}Ni_{0.2}Mn_{0.6}O_{1.95}$ show the spherical morphology of the precursor is preserved at high temperature. Moreover, we note that the agglomeration of the grains for $Li_{1.1}Ni_{0.2}Mn_{0.6}O_{1.95}$ powder synthesized by our preferred method is controlled by aging in the sealed container, which brings an improvement of the physical properties of the material.

[0039] In another preferred embodiment, morphology controlled $Li_{1.13}Ni_{0.3}Mn_{0.57}O_2$ was further coated with Lithium Lanthanum Titanium Oxides (LLTO) under different coating conditions in this experiment. These materials were made into Li coin cells. We compare the first cycle voltage profile of LNMO, #1 LLTO coated LNMO and #2 LLTO coated LNMO. The charge/discharge of first cycle were performed at 12.5 mA/g between 2V and 4.8V. The CE improved from 73.1% to 79.1% and 91.4%, respectively. To achieve the LLTO coating, $LiNO_3$/$LiCH_3COO$ (as lithium source), lanthanum nitrate hydrate (La(NO3)3·xH2O) (as lanthanum source), and titanium(IV) butoxide (Ti(OC4H9)O4)/$TiCl_4$ (as titanium source) were dissolved in ethanol or methanol or water. NH_4OH solution was added to the solution to adjust the pH to 9 to 11. Li excess powder was then added to the coating solution. Then the whole solution was transferred to a Teflon-sealed autoclave under thermal treatment at 80 to 90°C for 10 h to 15 h. The product was then dried at 100 °C under vacuum oven to

remove residual water and subsequently calcined at 700 or 900 °C for 5 h to 10h. The amount of LLTO is 1%-5 wt% of the Li excess material.

[0040] In another preferred embodiment, $Li_{1.144}Ni_{0.136}Co_{0.136}Mn_{0.544}O_{1.92}$ is obtained following the synthesis protocol described above with appropriate molar ratios of precursors. Sharp reflections in measured XRD patterns reveal the high crystallinity of the samples. SEM images for the $Li_{1.144}Ni_{0.136}Co_{0.136}Mn_{0.544}O_{1.92}$ show the spherical morphology of the precursor is preserved at high temperature. Moreover, we note that oxygen vacancies in the sample is determined by neutron diffraction (ND), a technique with high sensitivity for detecting light elements, such as Li and O. Electron energy loss spectroscopy (EELS) mapping reveals oxygen vacancies have been successfully introduced on the 0-20 nm of the surface without a noticeable interruption in the bulk-structure. Electrochemical measurements prove that surface oxygen vacancies introduction in Li excess cathodes without severe structural destruction has a considerable effect on improving electrochemical performance.

[0041] In another preferred embodiment, $Li_{1.18}Ni_{0.135}Co_{0.135}Mn_{0.539}Mo_{0.01}O_2$ is obtained following a the synthesis protocol described above with appropriate molar ratios of precursors.. Sharp reflections in measured XRD patterns reveal the high crystallinity of the samples. SEM images for the $Li_{1.18}Ni_{0.135}Co_{0.135}Mn_{0.539}Mo_{0.01}O_2$ show the spherical morphology of the precursor is preserved at high temperature (~~. Sample $Li_{1.18}Ni_{0.135}Co_{0.135}Mn_{0.539}Mo_{0.01}O_2$ synthesized by a preferred co-precipitation method shows a high discharge capacity (313 mAh/g) at 0.1 C rate and small irreversible capacity for the first cycle. Moreover, it exhibits almost the same capacity and voltage curve during cycling, which shows the preferred co-precipitation method with Mo doping holds promise for resolving the problem of the capacity and voltage fading during cycling of lithium-excess materials.

[0042] In additional preferred embodiments, lithium excess materials as described above are engineered to include oxygen vacancies. Preferred methods employ a gas-solid interface reaction to achieve delicate control of oxygen activity through uniformly creating oxygen vacancies without affecting structural integrity of Li-excess layered oxides, and thereby create lithium excess materials with uniform oxygen vacancies. Experiments showed that engineered lithium excess materials with uniform oxygen vacancies can deliver a discharge capacity as high as 301 mAh g^{-1} with initial Coulombic efficiency of 93.2%. After 100 cycles, a reversible capacity of 300 mAh g^{-1} still remains without any obvious decay in voltage. The methods demonstrate the ability to comprehensively design and control oxygen activity in layered oxide cathodes, which can greatly improve Li-ion batteries. In addition, the addition of oxygen vacancies via the methods of the invention does not affect the bulk properties of the Li excess material.

[0043] Preferred embodiments of the invention will now be discussed with respect to experiments. The experiments will be understood by artisans in view of the general knowledge in the art and the description that follows to demonstrate broader aspects of the invention.

[0044] Experiment 1.

[0045] $Li_{1.2}Ni_{0.2}Mn_{0.6}O_2$ (0.5 $LiNi_{0.5}Mn_{0.5}O_2$•0.5 Li_2MnO_3) is first obtained due to its high reversible discharge capacity (250 mAh g^{-1}) as well as relatively lower price (compare to Co contained materials). To make uniform spherical $Li_{1.2}Ni_{0.2}Mn_{0.6}O_2$ sample, precursor particles $(Ni_{0.25}Mn_{0.75})CO_3$ with homogenous composition were first synthesized via a preferred co-precipitation method.

[0046] An appropriate amount of Li_2CO_3 (the molar ratio of carbonate ions to transitional metal ions is 1:1 (1.05:1 to 1:1 and the actual amount is based on transition metal solution concentration)) was dissolved in 60 mL deionized water, and then added dropwise into 10 ml of a mixed solution of

$Ni(NO_3)_2$ and $Mn(NO_3)_2$ (Ni:Mn = 1:3 in molar ratio) under stirring. The resulting slurry was transferred to 100 mL Teflon lined stainless steel autoclave, and then aged at 80 °C for 12 h, the resulting $(Ni_{0.25}Mn_{0.75})CO_3$ precursor was washed several times by pure water to remove residual Li^+, and dried in a vacuum oven at 80 °C over night. Thereafter, the $(Ni_{0.25}Mn_{0.75})CO_3$ powder was mixed with a stoichiometric amount of Li_2CO_3, and was calcined at 500 °C for 5 h in a 50 ml porcelain crucible, and then heated up to 900 °C and kept at this temperature for 6 h followed by quenching in the air.

[0047] XRD has been used to confirm the obtained spherical sample is phase pure lithium-excess material. The XRD pattern of the $Li_{1.2}Ni_{0.2}Mn_{0.6}O_2$ sample is shown in FIG. 1. Sharp reflections in the XRD patterns reveal the high crystallinity of the sample. All XRD peaks in the pattern can be indexed as a hexagonal α-$NaFeO_2$ structure (space group: R-3m, NO. 166).

[0048] FIGs. 2A and 2B shows SEM images for the $Li_{1.2}Ni_{0.2}Mn_{0.6}O_2$ powder synthesized by the preferred co-precipitation method at 500nm and 10μm magnification scales. The images show that the obtained precursor has spherical morphology with particle sizes in the range of 2–3 μm. These micro-spherical particles are composed of primary particles with diameters of about 150 nm on average. Moreover, we note that the agglomeration of the grains for $Li_{1.2}Ni_{0.2}Mn_{0.6}O_2$ powder synthesized by our preferred method is controlled by aging in the sealed container, which provides the improved physical properties of the material, such as the specific surface area and tap density. The sample synthesized by the conventional method shows an agglomeration secondary particle with a large particle size distribution.

[0049] We have studied the effects of our morphology control process on the electrochemical performance of $Li_{1.2}Ni_{0.2}Mn_{0.6}O_2$ cathode materials. The first charge/discharge curves of the sample synthesized through a preferred

co-precipitation method are given in FIG. 3. When charged and discharged at a rate of 0.05 C between 2.0 V and 4.8 V, the sample can deliver a discharge capacity of about 250 mA h g^{-1}, which is consistent with the literature result for the same material.

[0050] FIGs. 4A and 4C compare cycling performance and FIGs. 4B and 4D discharge profiles for 20th, 40th, 60th and 80th cycles of a preferred sample $Li_{1.2}Ni_{0.2}Mn_{0.6}O_2$ under a current density of 25 mA g^{-1}, in the voltage range of 2.0–4.8 V to a sample lacking morphology control. Compared with the sample without morphology control (FIGs. 4C and 4D), the morphology control sample not only shows a large discharge capacity (220 mAh/g) at the first cycle, but also it exhibits almost the same capacity and voltage curve at the 80th cycle ((FIGs. 4A and 4B)), which shows the preferred co-precipitation method holds promise for resolving the problem of the capacity and voltage fading during cycling of lithium-excess materials.

[0051] Experiment 2.

[0052] Following the synthesis protocol in Experiment 1, $Li_{1.2}Ni_{0.136}Mn_{0.544}Co_{0.136}O_2$ is obtained in this experiment. The XRD pattern of the $Li_{1.2}Ni_{0.136}Mn_{0.544}Co_{0.136}O_2$ sample is shown in FIG. 5A. Sharp reflections in the XRD patterns reveal the high crystallinity of the samples. All XRD peaks in the two patterns can be indexed as a hexagonal α-$NaFeO_2$ structure (space group: *R-3m*, NO. 166), except for a few broad peaks between 20° and 25°. The diffraction peaks between 20° and 25° are known to be caused by the superlattice ordering of Li and Mn in the transition metal layers for the layered Li-excess oxides, which proves the existence of Li_2MnO_3 component.

[0053] FIGs. 5B and 5C are SEM images for the $Li_{1.2}Ni_{0.136}Mn_{0.544}Co_{0.136}O_2$ powder synthesized by the preferred co-precipitation method at respective 500nm and 10μm magnification scales. Even though the size of the primary particles increases to 150 nm due to the lithiation reaction and

crystal growth, the spherical morphology of the precursor is preserved at high temperature. Moreover, we note that the agglomeration of the grains for $Li_{1.2}Ni_{0.136}Mn_{0.544}Co_{0.136}O_2$ powder synthesized by our preferred method is controlled by aging in the sealed container, which is leveraged for the improvement of the physical properties of the material, including smaller secondary particle size that leads to less cracking and fewer voids. The tight structure with less void volume will improve the tap density as well as volumetric energy density of the battery.

[0054] FIG. 6 shows the first-cycle voltage profiles of $Li_{1.2}Ni_{0.136}Mn_{0.544}Co_{0.136}O_2$ cathode in the voltage range of 2–4.8 V under gravimetric current density of 25 mA/g (1 C = 250 mAh/g). The sample synthesized by co-precipitation method of the invention is composed of a slope region and a long plateau that is still at about 4.5V with a capacity at about 325 mAh/g. The slope region (<4.5 V) is attributed to the extraction of Li^+ ions from the lithium layer. After this process, the Ni^{2+} was oxidized to Ni^{4+}. The subsequent long plateau is caused by a concomitant loss of oxygen from the material lattice. This gives a high capacity in the subsequent cycling. The sample with Li_2CO_3 as precipitant shows a high discharge capacity (270 mAh/g) at 0.1 C rate and small irreversible capacity for the first cycle.

[0055] Experiment 3.

[0056] Following the synthesis protocol in Experiment 1, $Li_{1.1}Ni_{0.2}Mn_{0.6}O_{1.95}$ is obtained in this experiment. The XRD pattern of the $Li_{1.1}Ni_{0.2}Mn_{0.6}O_{1.95}$ sample is shown in FIG. 7A. Sharp reflections in the XRD patterns reveal the high crystallinity of the samples.

[0057] FIGs. 7B and 7C are SEM images for the $Li_{1.1}Ni_{0.2}Mn_{0.6}O_{1.95}$ powder synthesized by the preferred co-precipitation method at respective 500nm and 10μm magnification scales. The spherical morphology of the precursor is preserved at high temperature. Moreover, we note that the agglomeration

of the grains for $Li_{1.1}Ni_{0.2}Mn_{0.6}O_{1.95}$ powder synthesized by our preferred method is controlled by the aging.

[0058] Experiment 4

[0059] Morphology controlled $Li_{1.13}Ni_{0.3}Mn_{0.57}O_2$ was further coated with Lithium Lanthanum Titanium Oxides (LLTO) under different coating conditions in this experiment. FIG. 8A presents the XRD of LNMO before and after LLTO coating. As the inset figure indicates, the intensity of the LLTO peak depends on the coating conditions. These materials were made into Li coin cells. Figure x compares the first cycle voltage profile of LNMO, #1 LLTO coated LNMO and #2 LLTO coated LNMO. The charge/discharge of first cycle were performed at 12.5 mA/g between 2V and 4.8V. The CE improved from 73.1% to 79.1% and 91.4%, respectively.

[0060] The observed capacity was initially about 234 mAh g^{-1}, 231 mAh g^{-1}, and 222 mAh g^{-1} for LNMO, #1 LLTO coated LNMO and #2 LLTO coated LNMO at 12.5 mAh g^{-1}. FIGs. 8B-8D include date regarding the capacity versus cycles of these materials. The #1 LLTO coated LNMO shows 95.5% capacity retention after 200 cycles which is a better improvement than the LNMO pristine. The voltage profile showed in FIG. 8B indicates that with the help from the LLTO coating, there is less of a voltage fade This result suggests that the LLTO coating holds promise for eliminating LNMO's large initial irreversibility. Moreover, it also has the ability to maintain capacity and voltage retention.

[0061] Experiment 5

[0062] Following the similar synthesis protocol in Experiment 1, $Li_{1.144}Ni_{0.136}Co_{0.136}Mn_{0.544}O_{1.92}$ is obtained in this experiment. FIG. 9 illustrates time of flight neutron diffraction (ND) patterns for the sample. the lattice parameters of the sample are a = 2.8526(8) Å and c = 14.2503(7) Å. The oxygen occupancy is reduced to 96.21 ± 1.20%, which clearly shows oxygen vacancies formation of the sample.

[0063] FIG. 10 shows first charge-discharge profile of $Li_{1.144}Ni_{0.136}Co_{0.136}Mn_{0.544}O_{1.92}$ obtained from a commercially available 2016-type coin cell at 0.05 C-rate where 1.0 C-rate corresponds to the current density of 250 mA g^{-1}. The value of the initial discharge capacity for the sample can reach as high as 300 mAh g^{-1}. The initial coulombic efficiency also increases to 92.6%. Electrochemical measurements prove that surface oxygen vacancies introduction in Li excess cathodes without severe structural destruction has a considerable effect on improving electrochemical performance.

[0064] Experiment 6

[0065] Following the synthesis protocol in Experiment 1, $Li_{1.18}Ni_{0.135}Co_{0.135}Mn_{0.539}Mo_{0.01}O_2$ is obtained in this experiment. FIG. 11 shows first charge-discharge profile of $Li_{1.18}Ni_{0.135}Co_{0.135}Mn_{0.539}Mo_{0.01}O_2$ obtained from a 2016-type coin cell at 0.05 C-rate where 1.0 C-rate corresponds to the current density of 250 mA g^{-1}. The value of the initial discharge capacity for the sample can reach as high as 313 mAh g^{-1}. FIG. 11 also presents the cycling performance as well as discharge profiles of the sample $Li_{1.18}Ni_{0.135}Co_{0.135}Mn_{0.539}Mo_{0.01}O_2$ under a current density of 25 mA g^{-1}, in the voltage range of 2.0–4.8 V. Clearly, it exhibits almost the same capacity and voltage curve after cycling, which shows the preferred co-precipitation method with Mo doping holds promise for resolving the problem of the capacity and voltage fading during cycling of lithium-excess materials.

[0066] Table 1. Cycling performance summary results of the sample $Li_{1.2}Ni_{0.2}Mn_{0.6}O_2$: synthesized by the simplified co-precipitation method and conventional co-precipitation method without morphology control.

	1st dis. Capacity (mAh/g)	80th dis. Capacity (mAh/g)	Capacity retention
spherical	220	229	104%
Non-control	208	183	87%

[0067] Typically the preferred materials will only start fading after 100 cycles. The improved cycling performance of the sample synthesized by the preferred co-precipitation method can be attributed to two aspects of example preferred materials: (1) the morphology controlled sample has almost two times fold smaller surface area compared with the sample without morphology control, which will introduce less side reactions between released oxygen and the electrolyte species A thinner solid electrolyte interface layer is thus expected to form on the morphology controlled particles surface, that enables a minimized capacity and voltage fading during cycling process; (2) uniform distributed small secondary particles (~3 μm) increase material meso-structure stability so that no cracks can easily occur within the secondary particles, which will introduce less stress to the whole system.

[0068] Experiment 7

[0069] $Li[Li_{1.144}Ni_{0.136}Co_{0.136}Mn_{0.544}]O_2$ was synthesized in accordance with the above methods. Specifically, an aqueous solution containing $NiSO_4 \cdot 6H_2O$, $CoSO_4 \cdot 7H_2O$, and $MnSO_4 \cdot 4H_2O$ with a concentration of 2.0 mol L^{-1} was pumpted into a continuously stirred tank reactor (CSTR, capacity of 50 L); at the same time, a 2.0 mol L^{-1} Na_2CO_3 solution, and a 0.2 mol L^{-1} NH_4OH solution were added separately into the reactor. The co-precipitation temperature was held at 60 °C, and the pH value was fixed to 7.8. The resulting $(Ni_{1/6}Co_{1/6}Mn_{4/6})CO_3$ powders were washed several times with distilled water to remove residual Na^+, and dried in a vacuum oven at 80 °C for over 20h. The resulting precipitates were mixed with Li_2CO_3 and the exact molar ratio between them was 0.7. The mixed powders firstly were pre-treated at 500 °C for 5 h in the air and then calcinated at 850 °C for 15 h in the air. Then, they were cooled to room temperature in the furnace. The as-obtained sample was labeled pristine LR-NCM. This sample was

then treated to create oxygen vacancies as follows via a gas solid interface reaction (GSIR) process.

[0070] The GSIR process of the pristine LR-NCM sample with CO_2 was carried out as follows: a set amount of LR-NCM cathode materials and a given amount of NH_4HCO_3, which was as the precursor source of CO_2 after decomposition at certain temperatures, were placed in an enclosed reactor in an argon-filled glove box ($O_2 < 0.1$ ppm) with a total volume of 100 mL, and heated at 200 °C for 10 h. The optimal molar ratio between carbon dioxide and Li-excess layered oxides was about 1:5 (~1:5 to 2:5). It is important that the pristine LR-NCM cathode materials and the NH_4HCO_3 are separated physically in separate containers at the beginning for ensuring a homogeneous gas-solid interface reaction. To remove the reaction products on the surface of the LR-NCM, the sample obtained was washed with water several times and dried at 120 °C for 12h. The as-obtained product was termed the GSIR LR-NCM. These procedures have been duplicated to demonstrate the GSIR process. The CO_2 released from the precursor under high temperature treatment will react with lattice oxygen in the powder to form Li_2CO_3 on the surface. This creates oxygen vacancies.

[0071] The produced GSIR LR-NCM materials were characterized and showed no significant change in crystal structure compared to the untreated pristine LR-NCM. This showed that the GSIR process does not heavily influence the average crystal structures and bulk electronic environments. This is shown in FIGs. 12A and 12B, which include time of flight neutron diffraction (ND) patterns for the pristine and GSIR LR-NCM. The oxygen vacancy for the GSIR LR-NCM is around three percent higher than that of the pristine LR-NCM sample.

[0072] Commercially available CR2032 coin-cells with metallic Li as the counter electrode were assembled to investigate the electrochemical performance of

the pristine and GSIR LR-NCM samples. Similar to other Li-excess layered oxides, both of them (FIG. 13A) exhibit a long plateau region at ~ 4.5 V *vs.* Li^+/Li^0, which usually is ascribed to the electrochemical activation of the Li_2MnO_3 component during the initial charge process, although an electrolyte/electrode side reaction is expected in this region. Interestingly, the value of the initial discharge capacity for the GSIR LR-NCM can reach as high as 301 mAh g^{-1} compared to that of 276 mAh g^{-1} for the pristine LR-NCM. The initial coulombic efficiency also increases from 83.8% to 93.2%. The corresponding differential capacity *vs.* voltage (*dQ/dV*) curves are plotted in FIG. 13B. At all tested rates, the GSIR LR-NCM exhibits a higher capacity than that of the pristine LR-NCM. Additional testing showed that the GSIR LR-NCM delivers a higher discharge-capacity of 298 mAh g^{-1} when it returns to the 0.1 C-rate, compared to that of 288 mAh g^{-1} for the pristine LR-NCM. Moreover, the GSIR LR-NCM demonstrate a slight degradation in potential after 100 cycles, even for a discharge capacity as high as 300 mAh g^{-1}.

[0073] While specific embodiments of the present invention have been shown and described above and the attachment following the claims, it should be understood that other modifications, substitutions and alternatives are apparent to one of ordinary skill in the art. Such modifications, substitutions and alternatives can be made without departing from the spirit and scope of the invention.

[0074] Various features of the invention are set forth in the appended claims.

CLAIMS

1. A lithium-excess cathode material comprising $Li_{1+x}Ni_aMn_bCo_cMo_dO_{2-y}$ ($0<x<0.3$, $0\leq a\leq 1$, $0\leq b\leq 1$, $0\leq c\leq 1$, $0\leq d\leq 0.2$, $0\leq y\leq 0.25$) in the form of secondary spherical microparticles formed from primary spherical nanoparticles.

2. The material of claim 1, further comprising excess oxygen vacancies in the material.

3. The material of claims 1 or 2, comprising $Li_{1.2}Ni_{0.2}Mn_{0.6}O_2$.

4. The material of claims 1 or 2, comprising $Li_{1.2}Ni_{0.136}Mn_{0.544}Co_{0.136}O_2$.

5. The material of claims 1 or 2, comprising $Li_{1.1}Ni_{0.2}Mn_{0.6}O_{1.95}$.

6. The material of claims 1 or 2, comprising $Li_{1.13}Ni_{0.3}Mn_{0.57}O_2$.

7. The material of claims 1 or 2, comprising $Li_{1.144}Ni_{0.136}Co_{0.136}Mn_{0.544}O_{1.92}$.

8. The material of claims 1 or 2, comprising $Li_{1.18}Ni_{0.135}Co_{0.135}Mn_{0.539}Mo_{0.01}O_2$.

9. The material of any of claims 1-8 further comprising a lithium lanthanum titanium oxide coating.

10. The material of any of claims 1-9, wherein the secondary spherical particles are ~2–3 μm.

11. The material of any of claims 1-10, wherein the primary nanoparticles are ~130nm to 170nm.

12. The material of any of claims 1-11, as part of a cathode in a lithium ion battery.

13. The electrode material of claim 1 where $0<x<0.3$, $0\leq a\leq 1$, $0\leq b\leq 1$, $0\leq c\leq 1$, $0\leq d\leq 0.2$, $0\leq y\leq 0.25$.

14. A method for forming morphology controlled lithium-excess cathode material, comprising:

mixing a carbonates or hydroxides solution into a mixed solution of transition metal (M) ions with predetermined stoichiometry under stirring;

aging resulting transition metal carbonates or hydroxides at a predetermined temperature for period of time to produce primary nanoparticles of a predetermined size;

washing and then drying a resulting powder;

mixing the powder with a stoichiometric amount of lithium carbonate or lithium hydroxide;

calcinating the mixture to produce the morphology controlled lithium-excess cathode material having secondary nanoparticles of a predetermined size.

15. The method of claim 14, wherein said resulting powder comprises $Li_{1.2}Ni_{0.2}Mn_{0.6}O_2$ ($0.5\ LiNi_{0.5}Mn_{0.5}O_2 \bullet 0.5\ Li_2MnO_3$).

16. The method of claim 14, further comprising coating the mixture with a lithium lanthanum titanium oxide coating.

17. The method of claim 14, further comprising introducing oxygen vacancies into the morphology controlled lithium-excess cathode material via gas solid interfacial modification.

18. The method of claim 17, wherein said gas solid interfacial modification comprises placing the lithium-excess cathode material and a CO_2 precusor separate from each other and heating to induce the gas solid interfacial modification and create excess oxygen vacancy morphology controlled lithium-excess cathode material.

19. The method of claim 18, wherein the CO_2 precusor comprises NH_4HCO_3.

20. The method of claim 19, further comprising washing the oxygen vacancy morphology controlled lithium-excess cathode material.

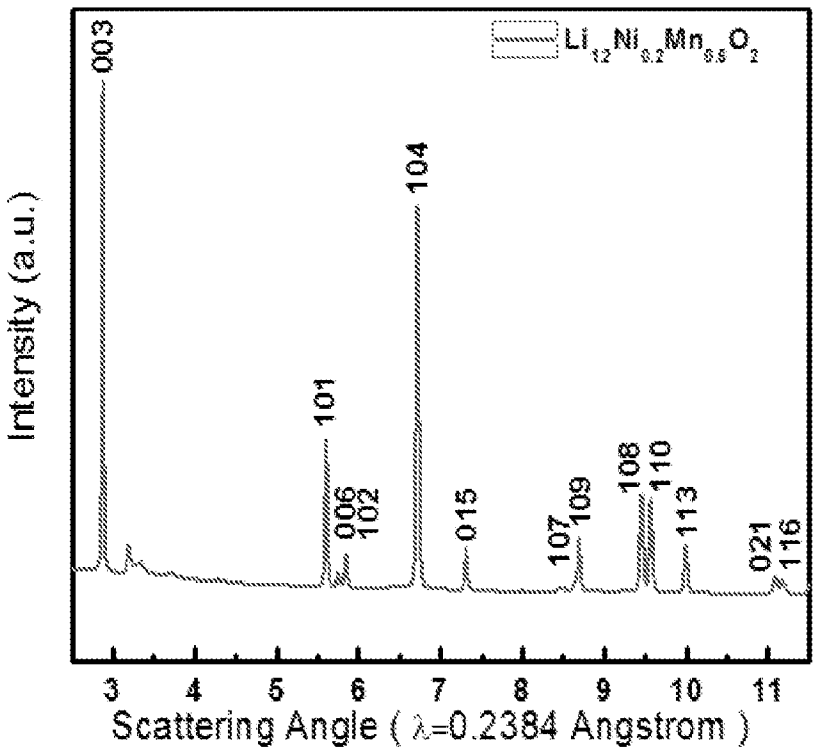
Li1.2Ni0.2Mn0.6O2
003
101
006
102
104
015
107
109
108
110
113
021
116
Intensity (a.u.)
3
4
5
6
7
8
9
10
11
Scattering Angle (λ=0.2384 Angstrom)

FIG. 1

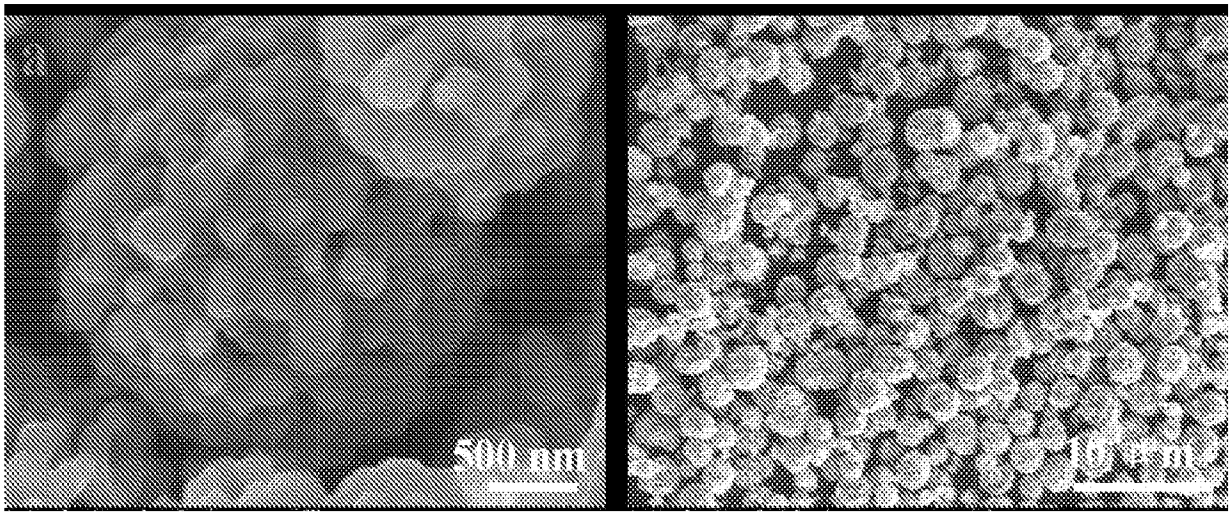

FIG. 2A FIG. 2B

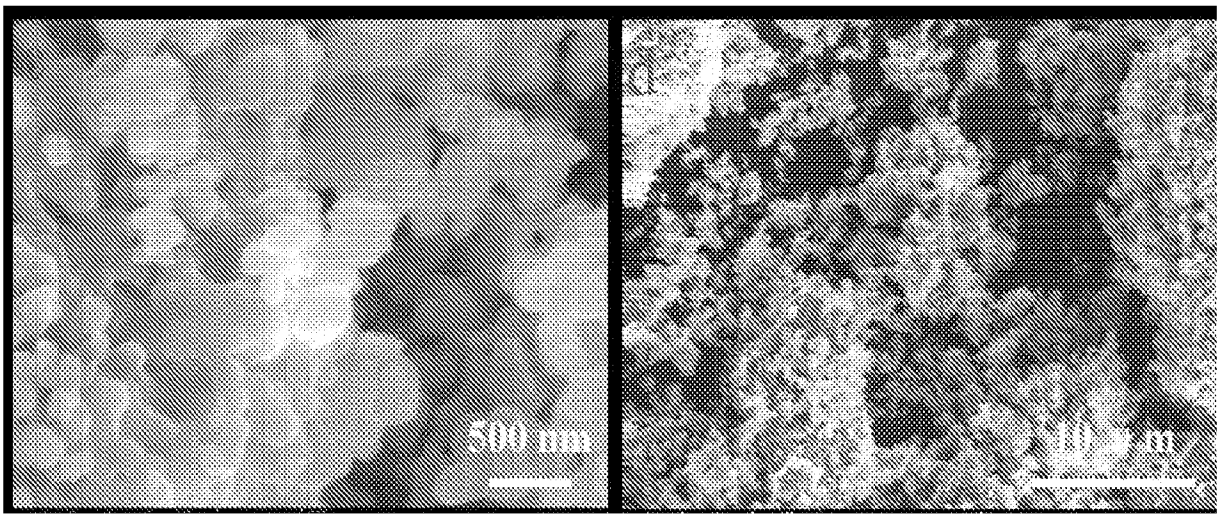

FIG. 2C FIG. 2D

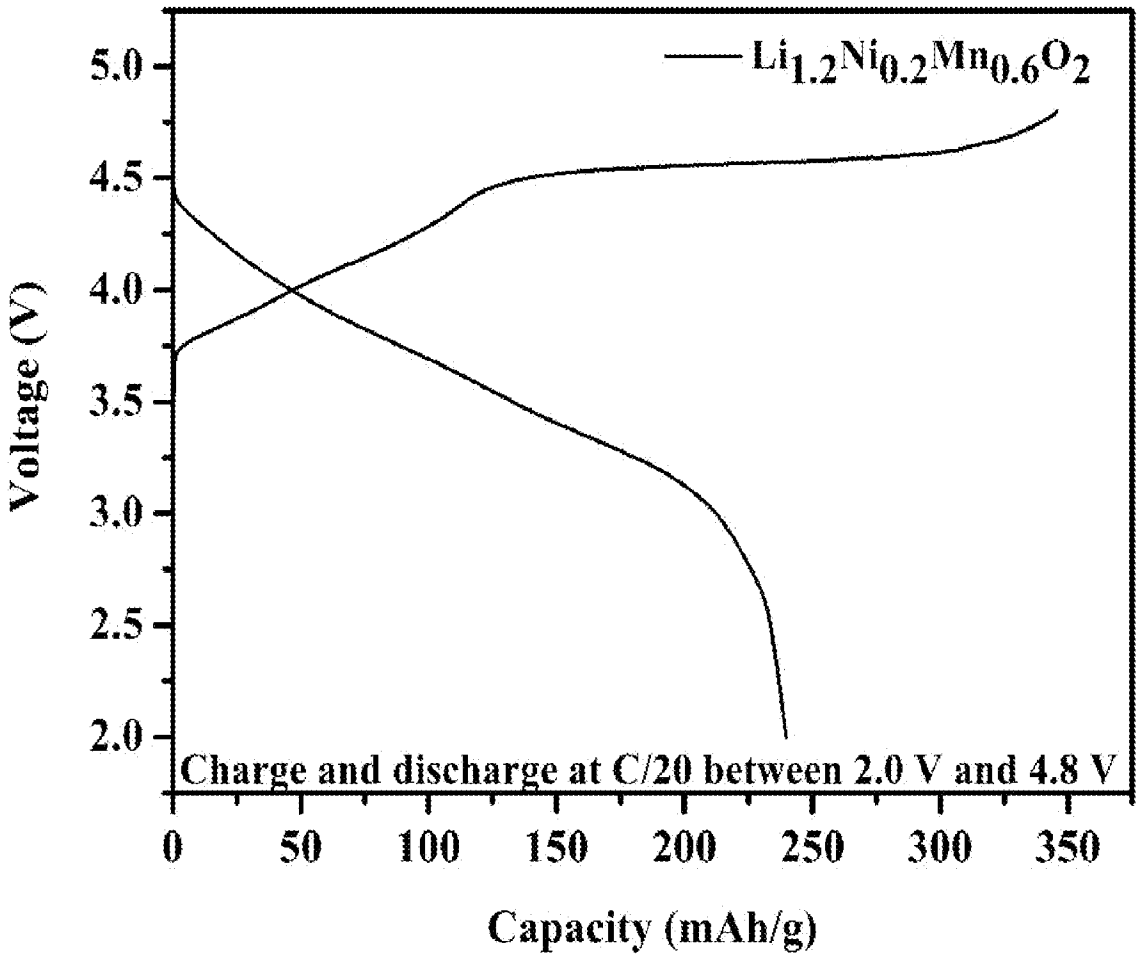
$Li_{1.2}Ni_{0.2}Mn_{0.6}O_2$
Voltage (V)
5.0
4.5
4.0
3.5
3.0
2.5
2.0
Charge and discharge at C/20 between 2.0 V and 4.8 V
0
50
100
150
200
250
300
350
Capacity (mAh/g)

FIG. 3

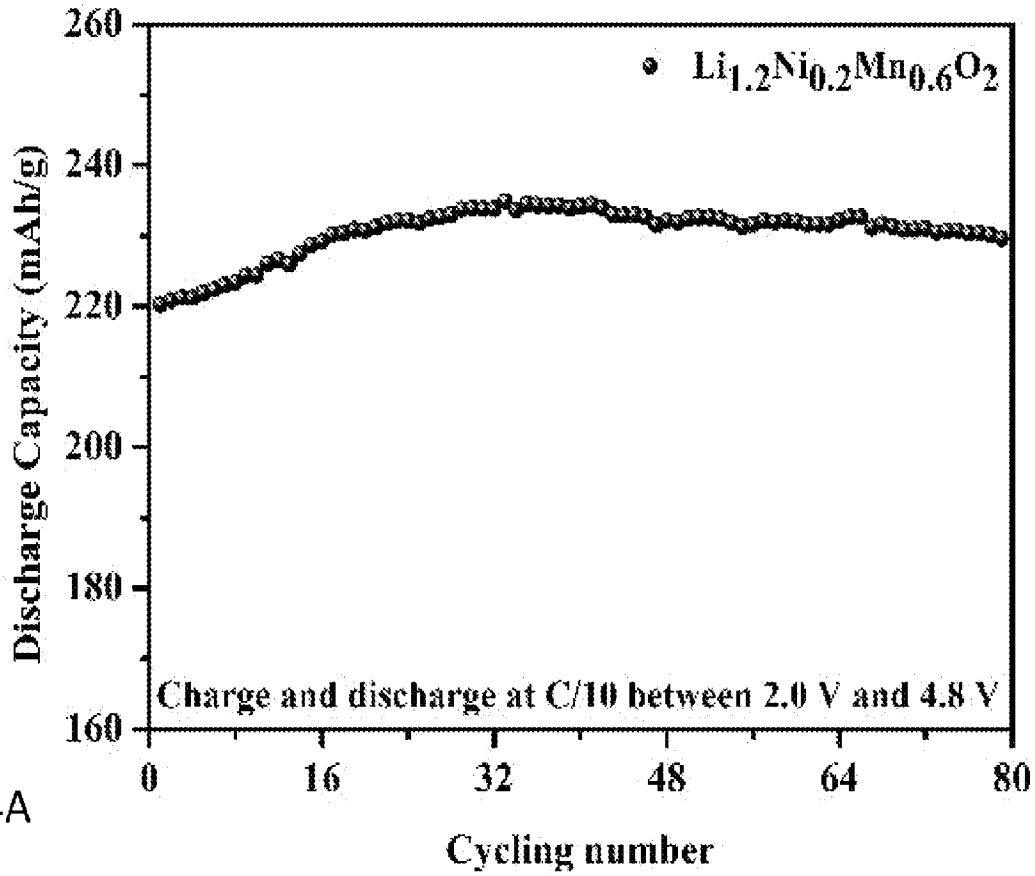
260
240
220
200
180
160
Discharge Capacity (mAh/g)
$Li_{1.2}Ni_{0.2}Mn_{0.6}O_2$
Charge and discharge at C/10 between 2.0 V and 4.8 V
0
16
32
48
64
80
Cycling number

FIG. 4A

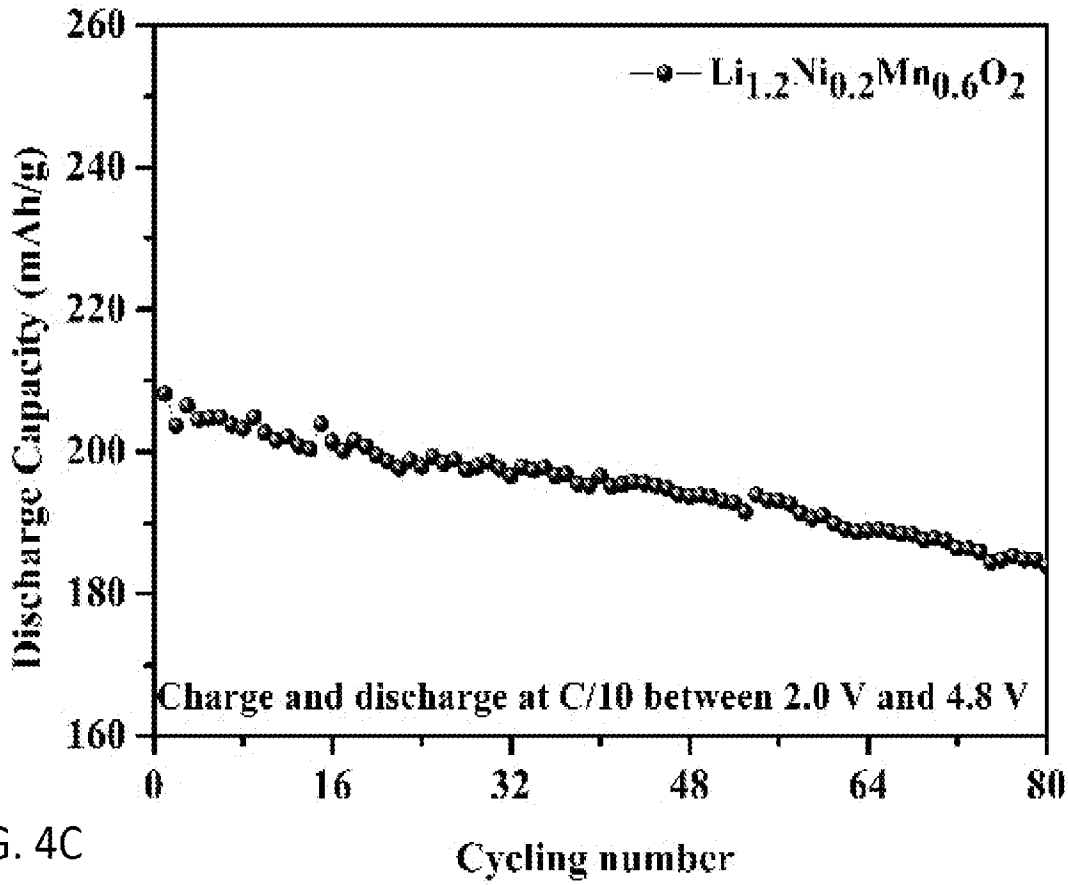
260
240
220
200
180
160
Discharge Capacity (mAh/g)
$Li_{1.2}Ni_{0.2}Mn_{0.6}O_2$
Charge and discharge at C/10 between 2.0 V and 4.8 V
0
16
32
48
64
80
Cycling number

FIG. 4C

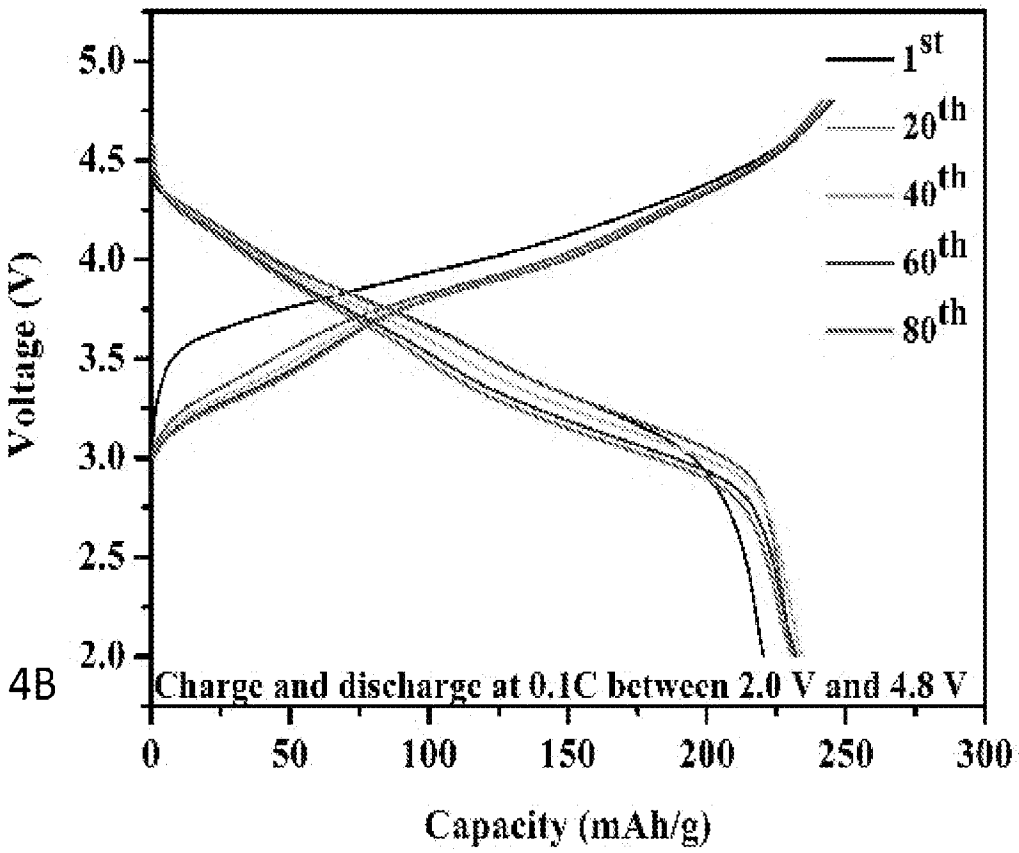
Voltage (V)
5.0
4.5
4.0
3.5
3.0
2.5
2.0
1st
20th
40th
60th
80th
Charge and discharge at 0.1C between 2.0 V and 4.8 V
0
50
100
150
200
250
300
Capacity (mAh/g)

FIG. 4B

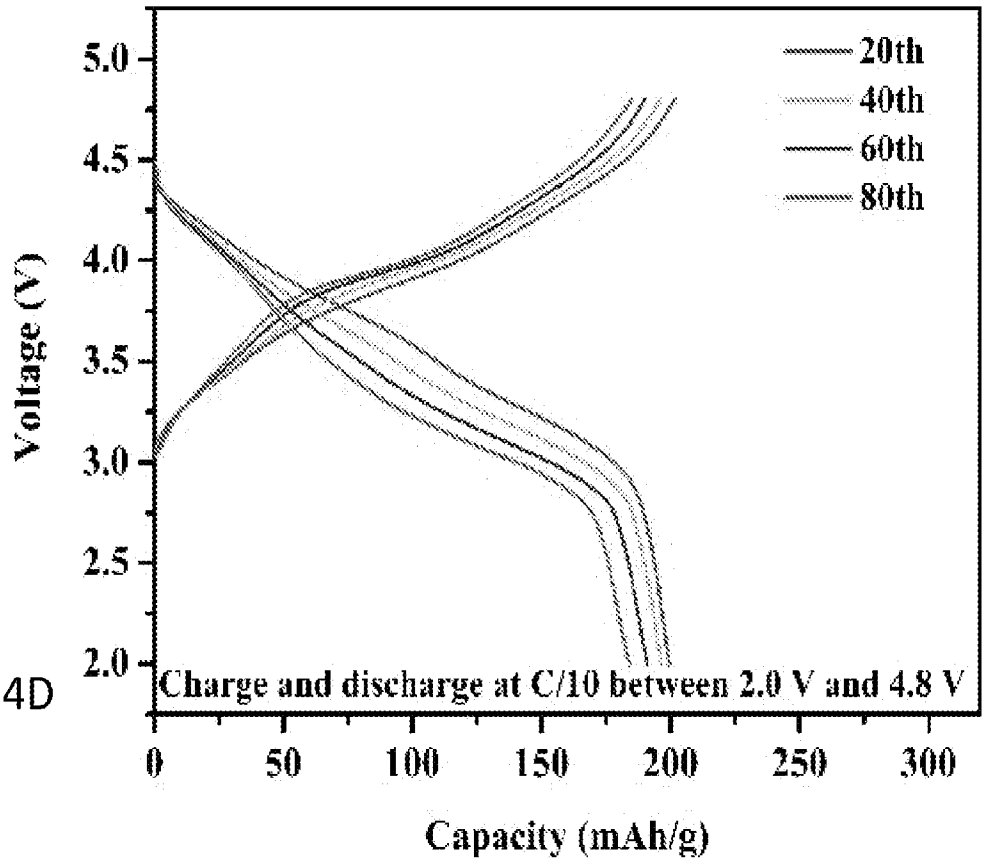
Voltage (V)
5.0
4.5
4.0
3.5
3.0
2.5
2.0
20th
40th
60th
80th
Charge and discharge at C/10 between 2.0 V and 4.8 V
0
50
100
150
200
250
300
Capacity (mAh/g)

FIG. 4D

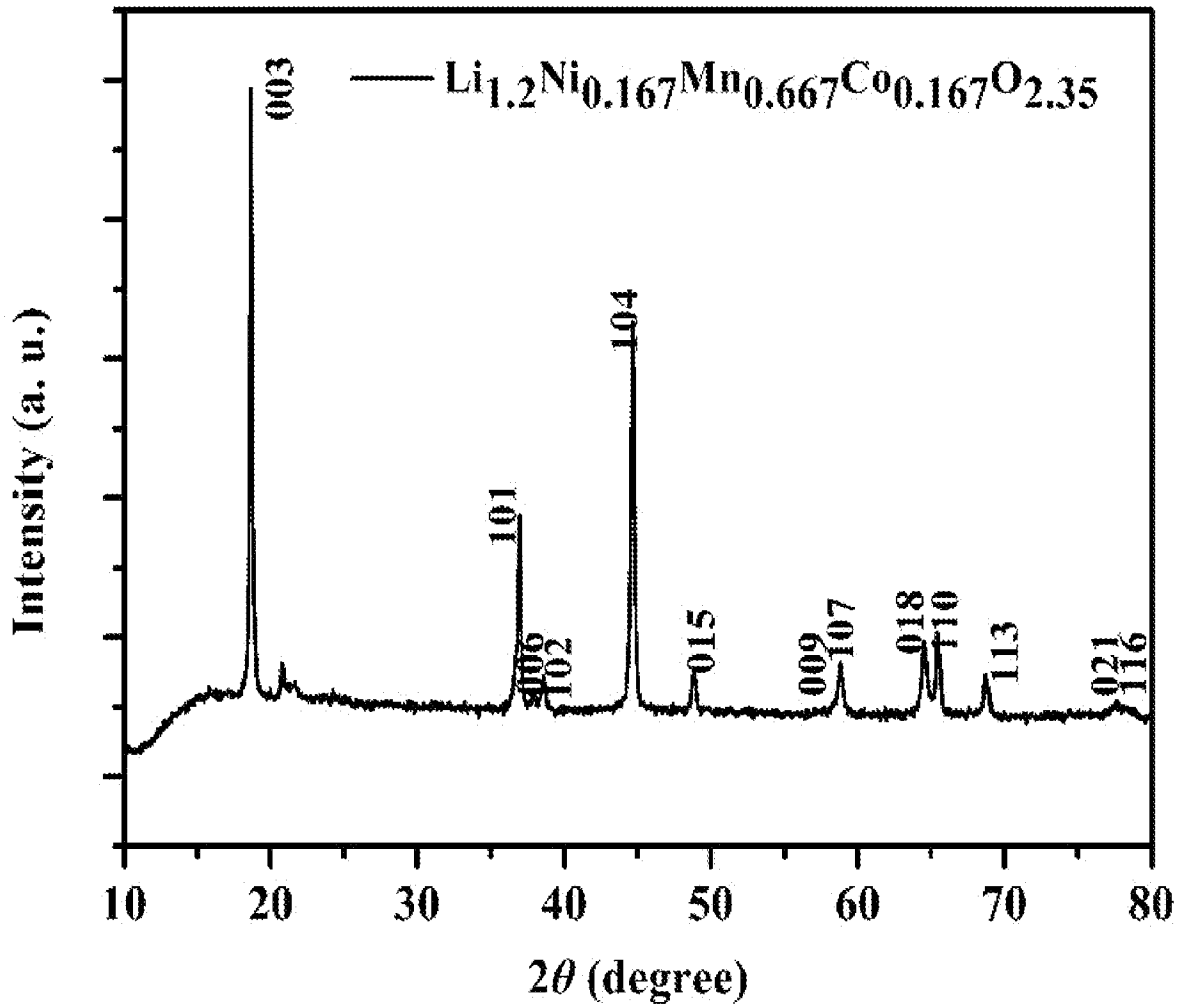
Li1.2Ni0.167Mn0.667Co0.167O2.35
003
101
006
102
104
015
009
107
018
110
113
021
116
Intensity (a. u.)
10
20
30
40
50
60
70
80
2θ (degree)

FIG. 5A

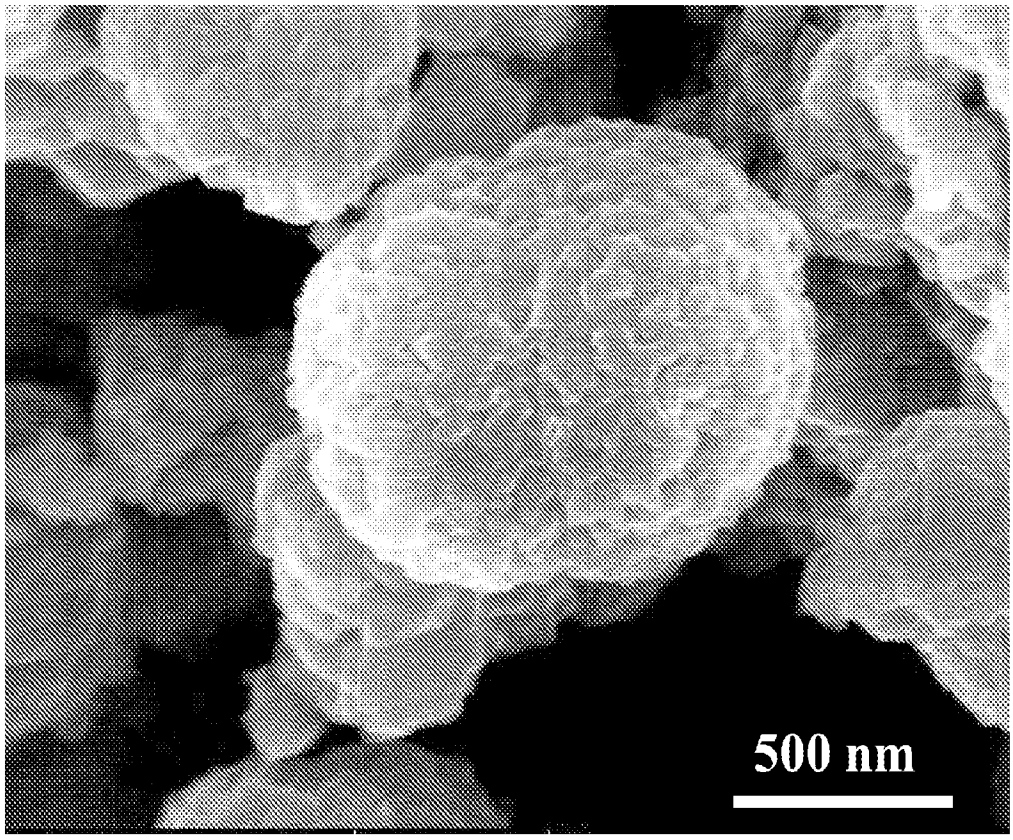

FIG. 5B

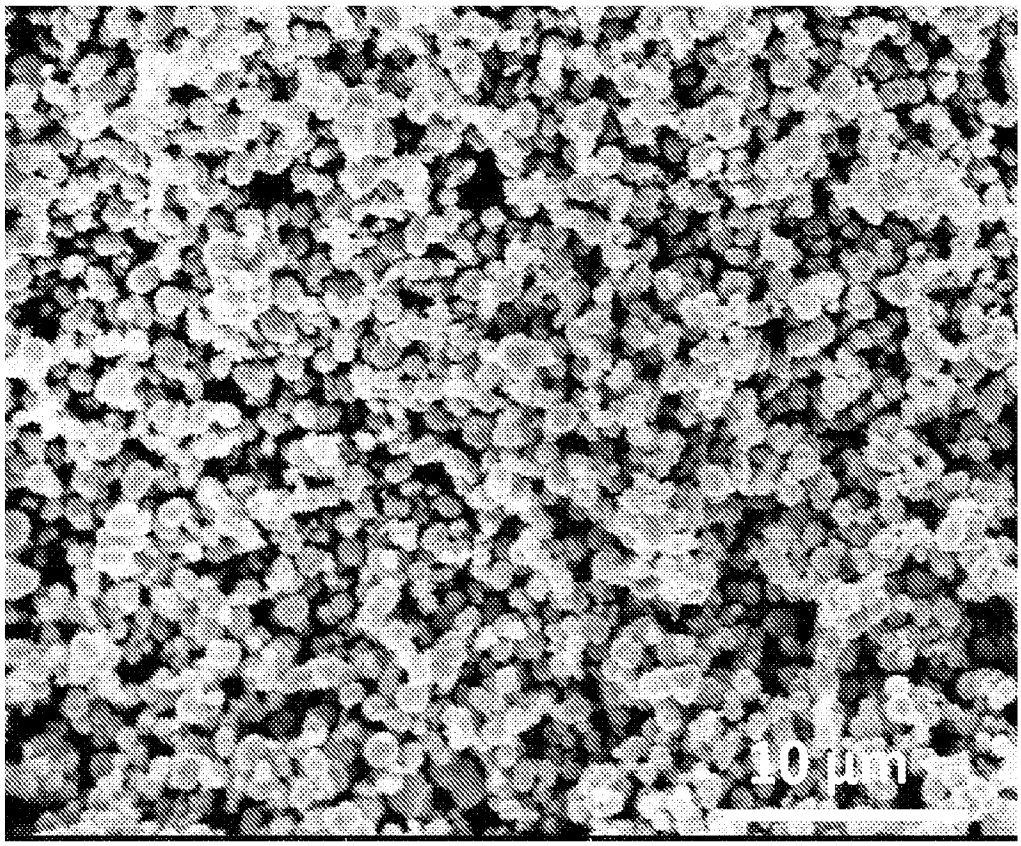

FIG. 5C

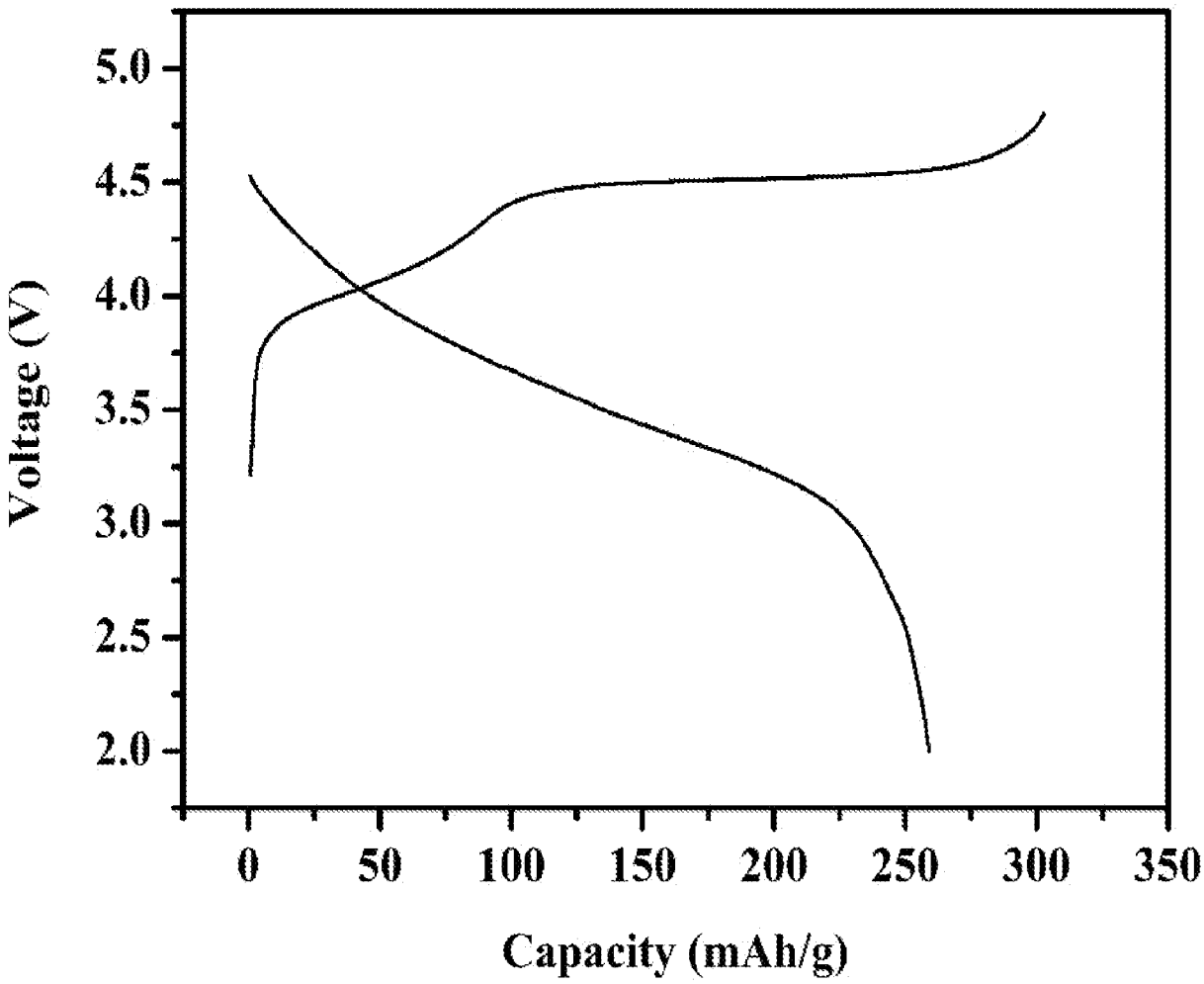
5.0
4.5
4.0
3.5
3.0
2.5
2.0
Voltage (V)
0
50
100
150
200
250
300
350
Capacity (mAh/g)

FIG. 6

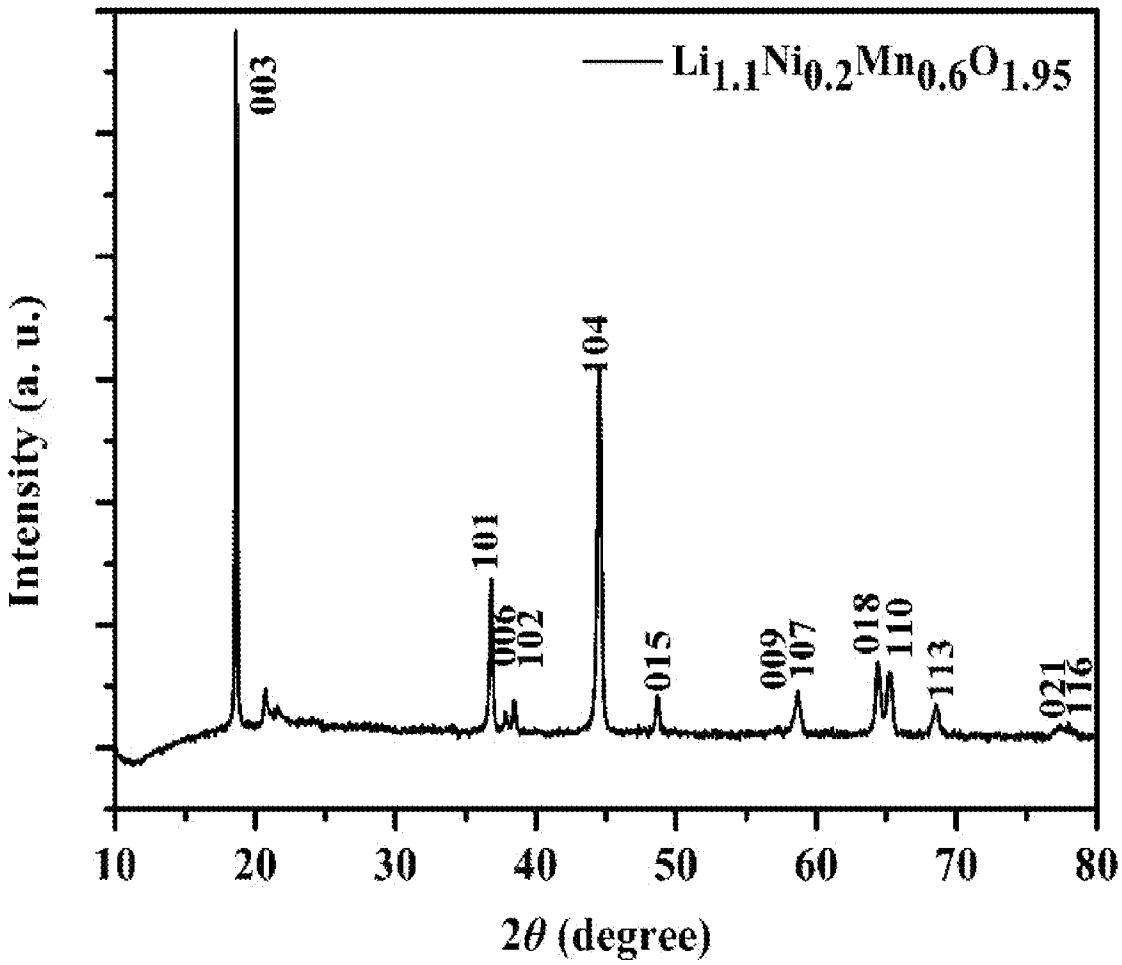
Li1.1Ni0.2Mn0.6O1.95
003
101
006
102
104
015
009
107
018
110
113
021
116
Intensity (a. u.)
10
20
30
40
50
60
70
80
2θ (degree)

FIG. 7A

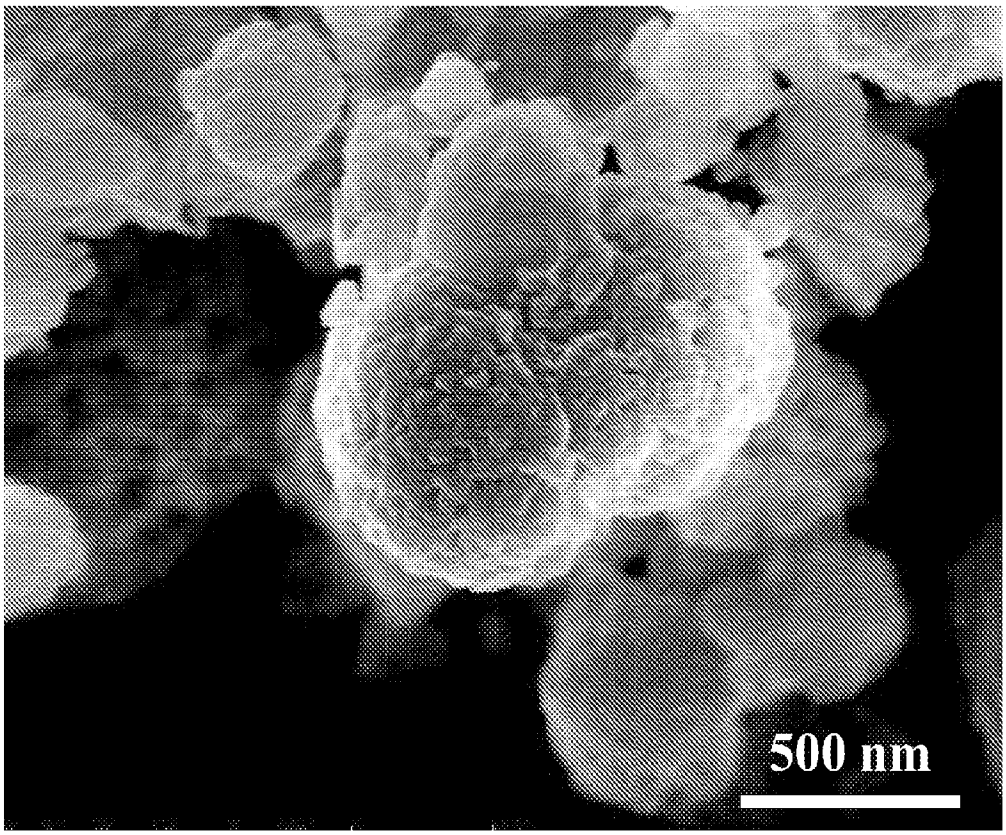

FIG. 7B

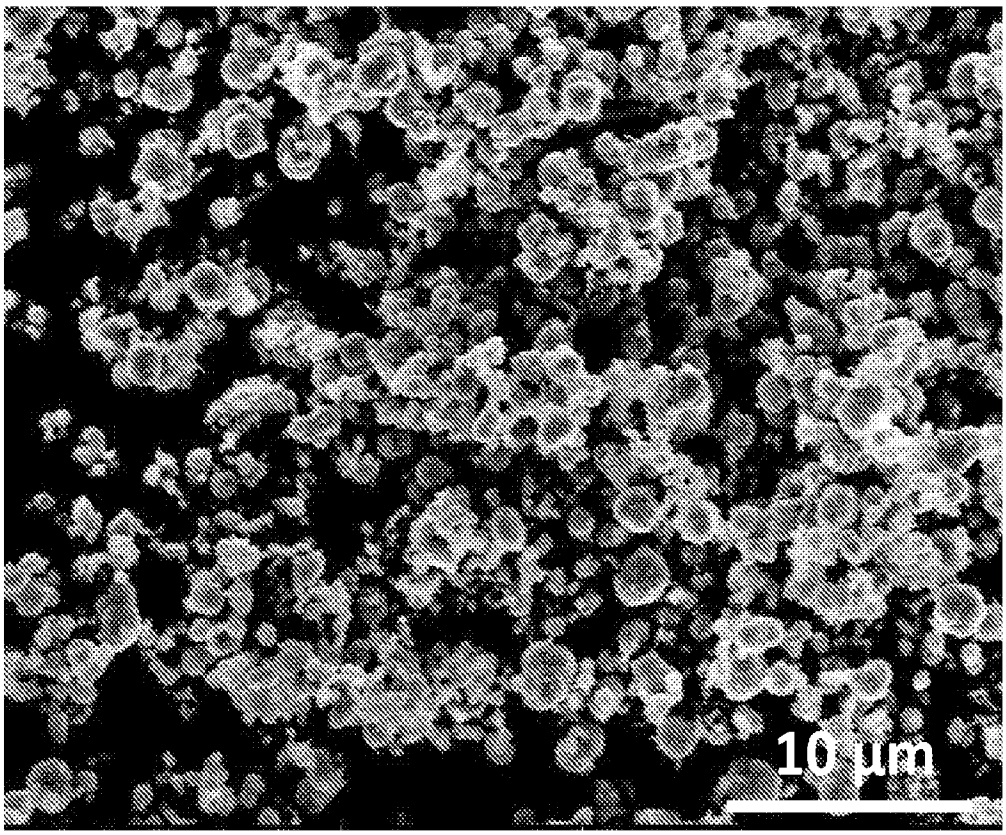

FIG. 7C

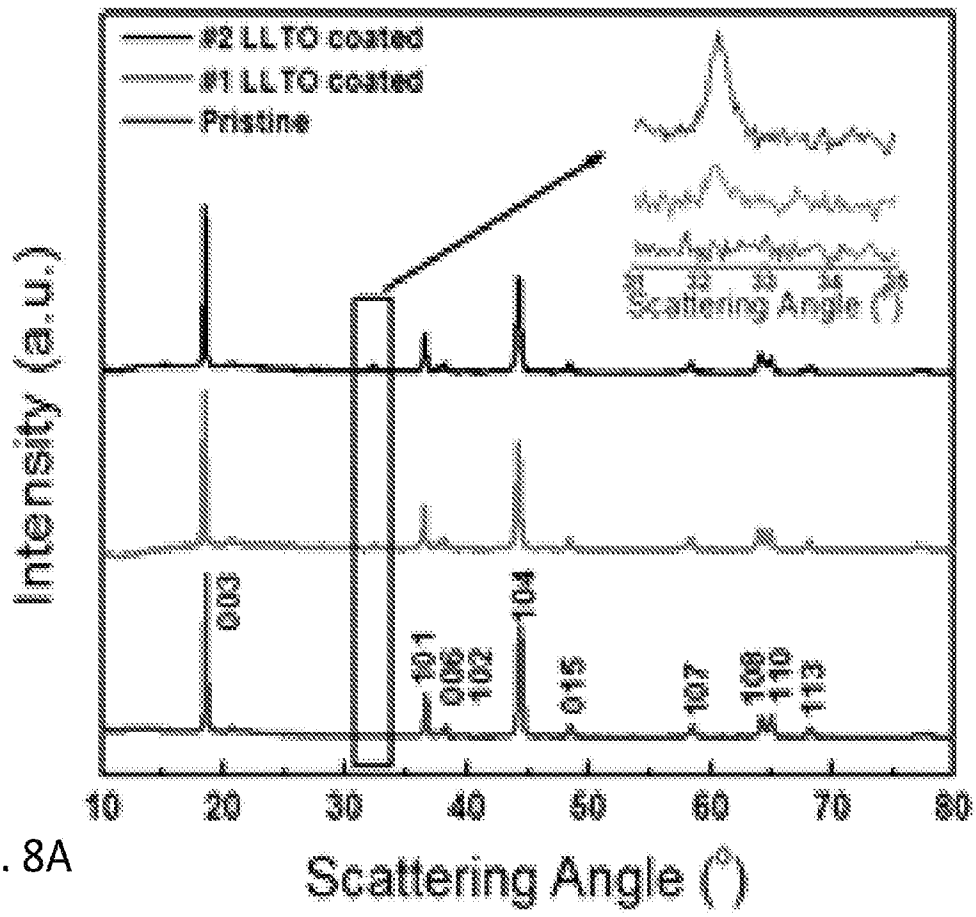
#2 LLTO coated
#1 LLTO coated
Pristine
Intensity (a.u.)
003
101
006
102
104
015
107
108
110
113
10
20
30
40
50
60
70
80
Scattering Angle (°)

FIG. 8A

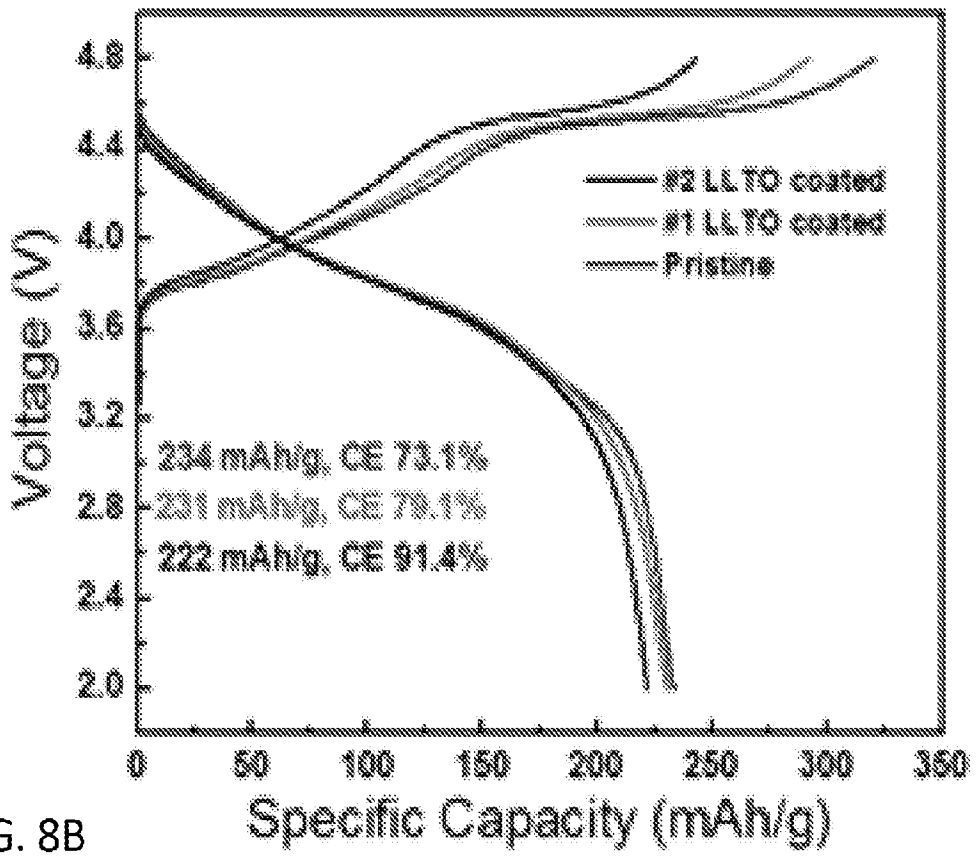
#2 LLTO coated
#1 LLTO coated
Pristine
234 mAh/g, CE 73.1%
231 mAh/g, CE 78.1%
222 mAh/g, CE 91.4%
Voltage (V)
4.8
4.4
4.0
3.6
3.2
2.8
2.4
2.0
0
50
100
150
200
250
300
350
Specific Capacity (mAh/g)

FIG. 8B

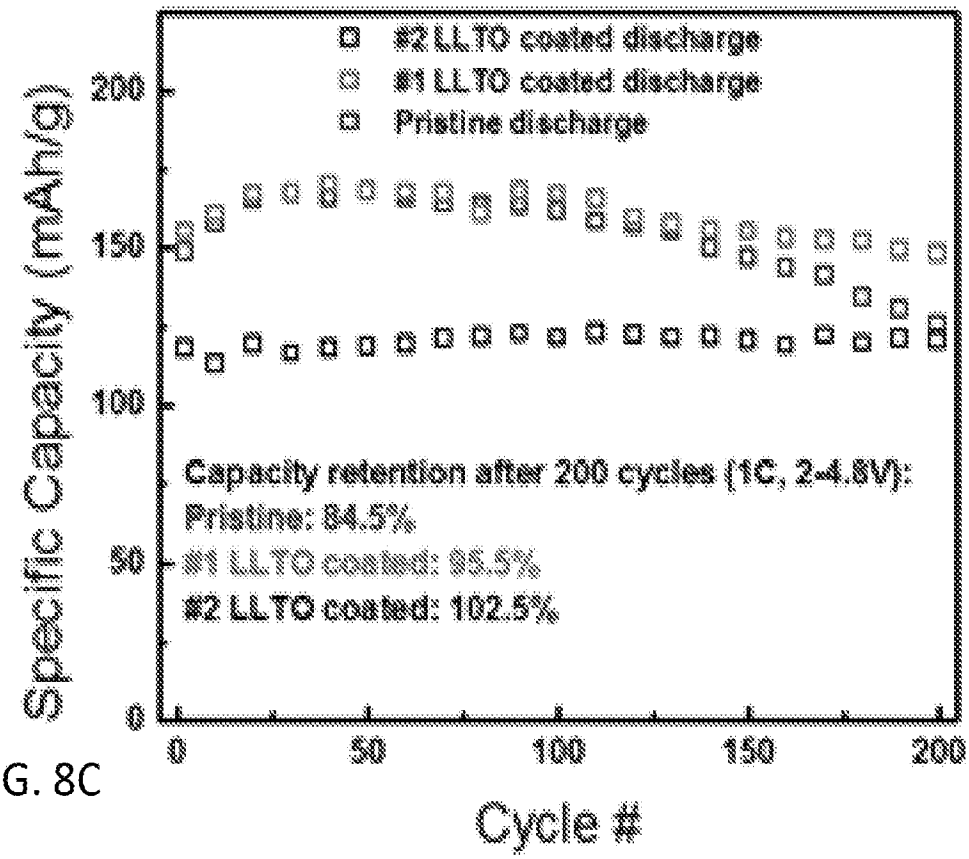
#2 LLTO coated discharge
#1 LLTO coated discharge
Pristine discharge
Capacity retention after 200 cycles (1C, 2-4.8V):
Pristine: 84.5%
#1 LLTO coated: 95.5%
#2 LLTO coated: 102.5%
Specific Capacity (mAh/g)
Cycle #
0
50
100
150
200

FIG. 8C

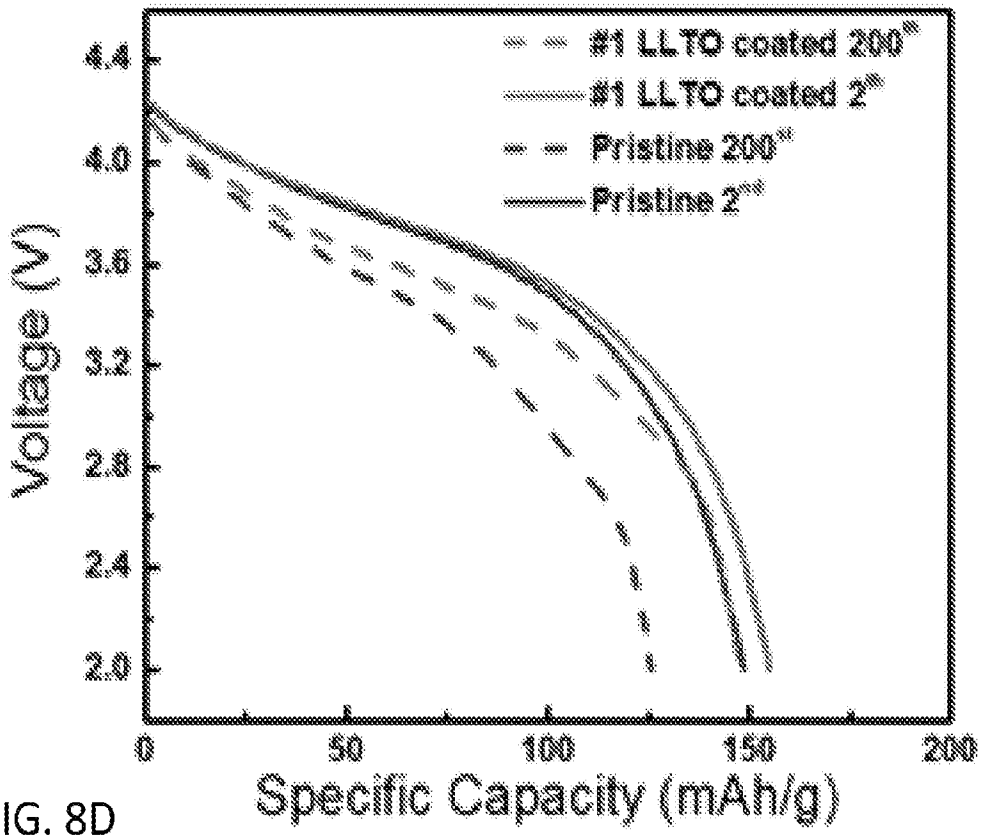
#1 LLTO coated 200th
#1 LLTO coated 2nd
Pristine 200th
Pristine 2nd
Voltage (V)
Specific Capacity (mAh/g)
4.4
4.0
3.6
3.2
2.8
2.4
2.0
0
50
100
150
200

FIG. 8D

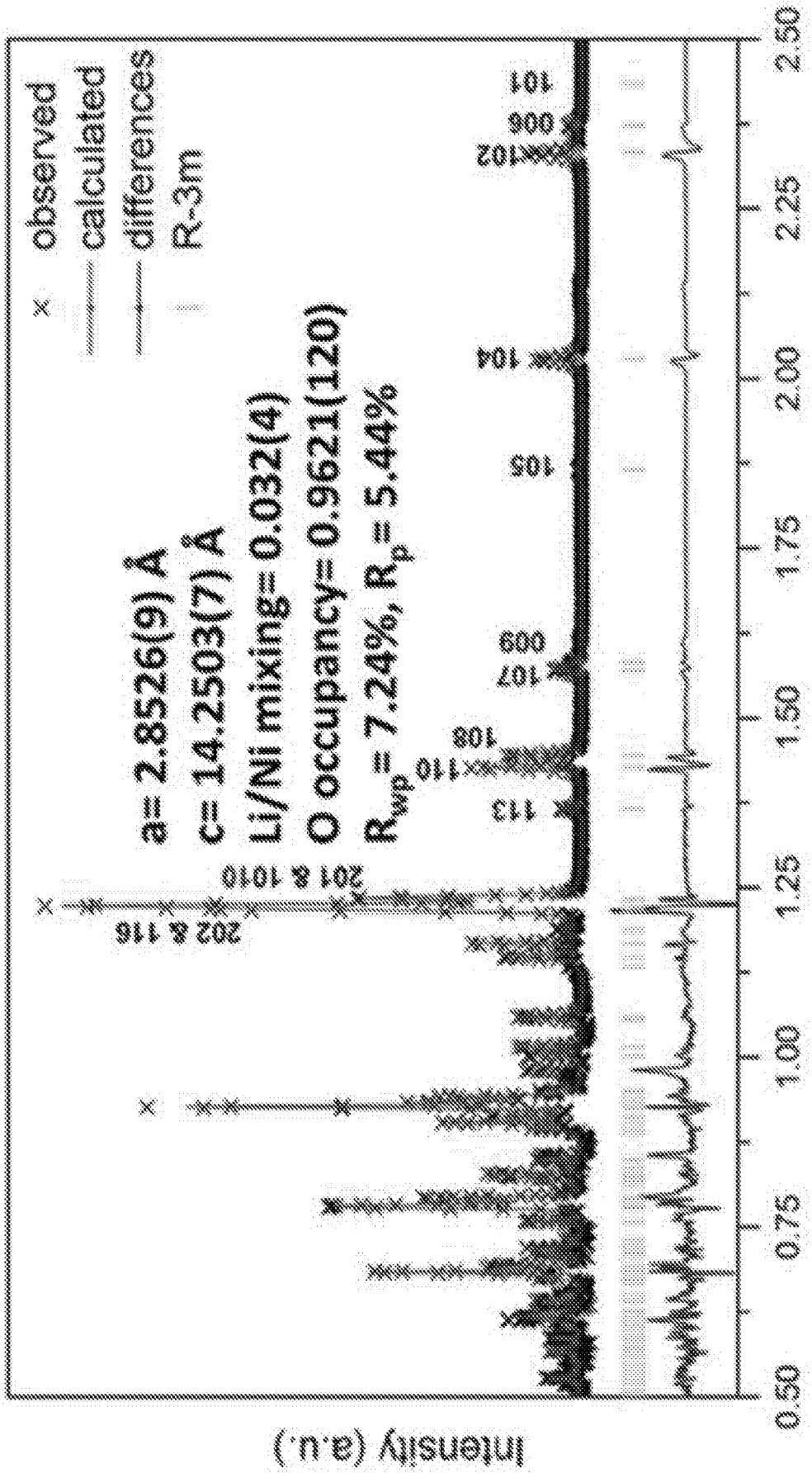
observed
calculated
differences
R-3m
a= 2.8526(9) Å
c= 14.2503(7) Å
Li/Ni mixing= 0.032(4)
O occupancy= 0.9621(120)
R_{wp} = 7.24%, R_p = 5.44%
003
101
006
102
104
105
107
108
110
113
201 & 1010
202 & 116
Intensity (a.u.)
0.50
0.75
1.00
1.25
1.50
1.75
2.00
2.25
2.50
d spacing (Angstrom)

FIG. 9

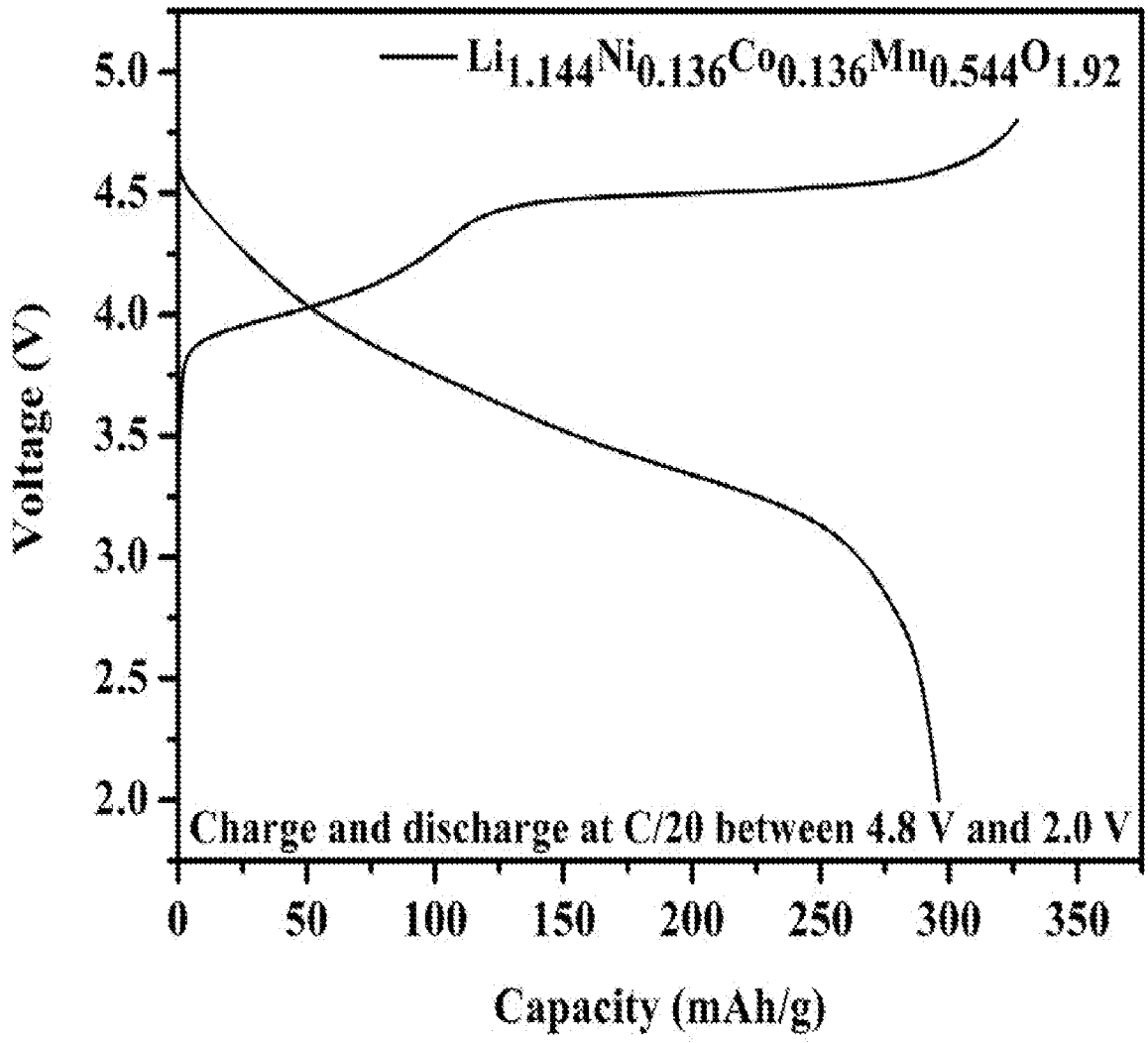
$Li_{1.144}Ni_{0.136}Co_{0.136}Mn_{0.544}O_{1.92}$
Voltage (V)
5.0
4.5
4.0
3.5
3.0
2.5
2.0
Charge and discharge at C/20 between 4.8 V and 2.0 V
0
50
100
150
200
250
300
350
Capacity (mAh/g)

FIG. 10

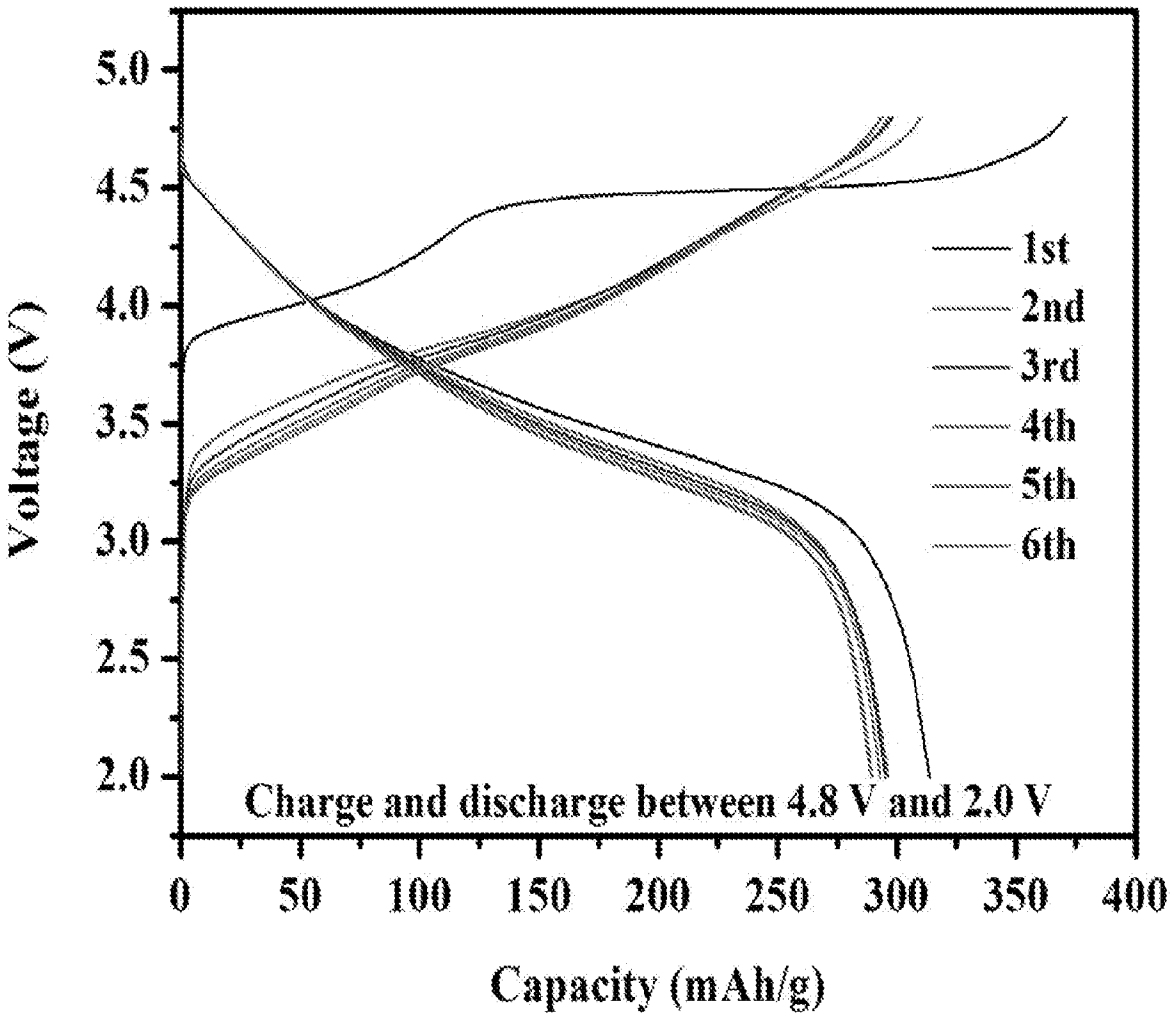
Voltage (V)
5.0
4.5
4.0
3.5
3.0
2.5
2.0
0
50
100
150
200
250
300
350
400
Capacity (mAh/g)
1st
2nd
3rd
4th
5th
6th
Charge and discharge between 4.8 V and 2.0 V

FIG. 11

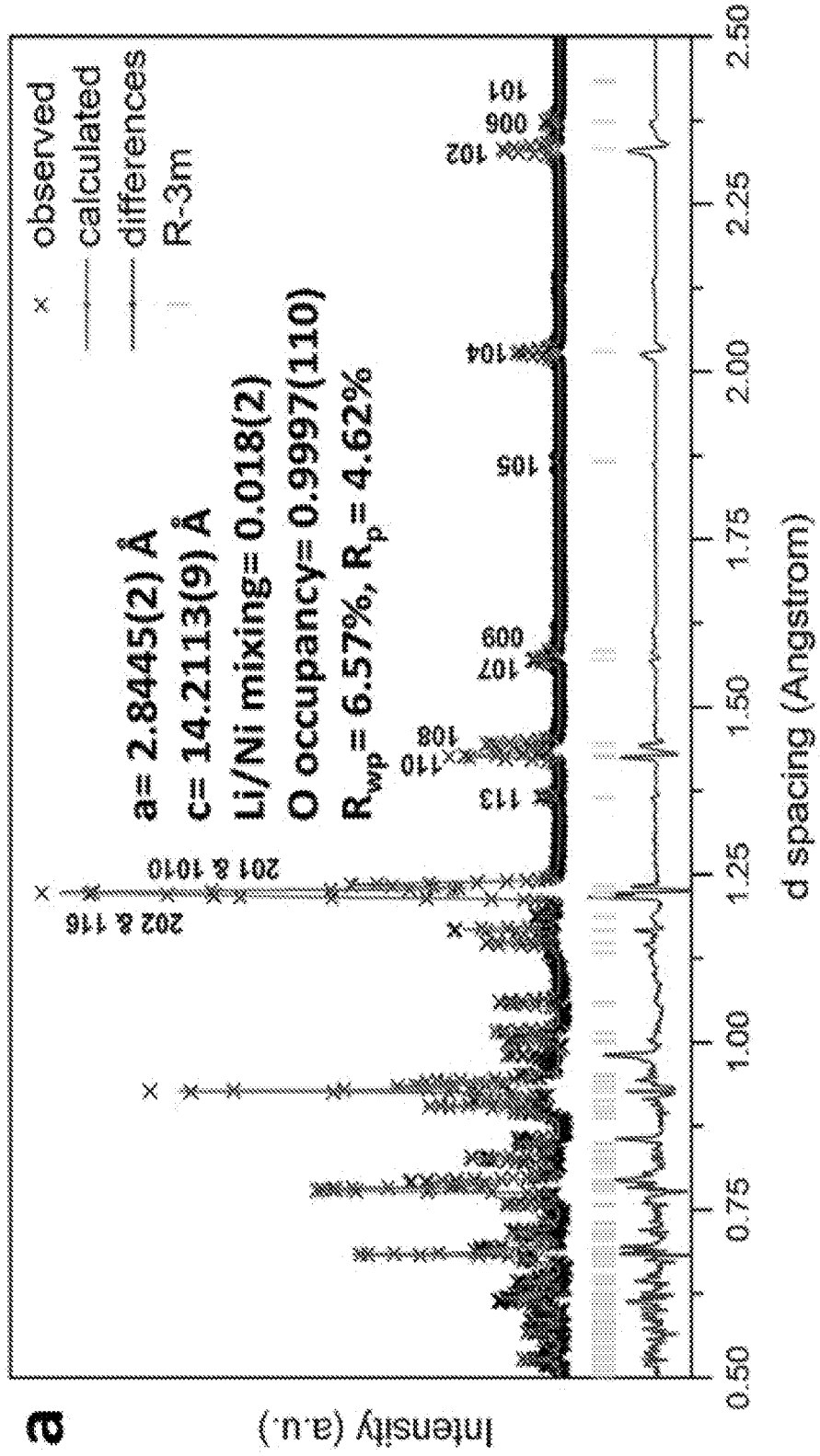
a
Intensity (a.u.)
d spacing (Angstrom)
0.50
0.75
1.00
1.25
1.50
1.75
2.00
2.25
2.50
× observed
calculated
differences
R-3m
a= 2.8445(2) Å
c= 14.2113(9) Å
Li/Ni mixing= 0.018(2)
O occupancy= 0.997(110)
R_{wp}= 6.57%, R_p= 4.62%
202 & 116
201 & 1010
113
110
108
107
009
105
104
102
006
101

FIG. 12A

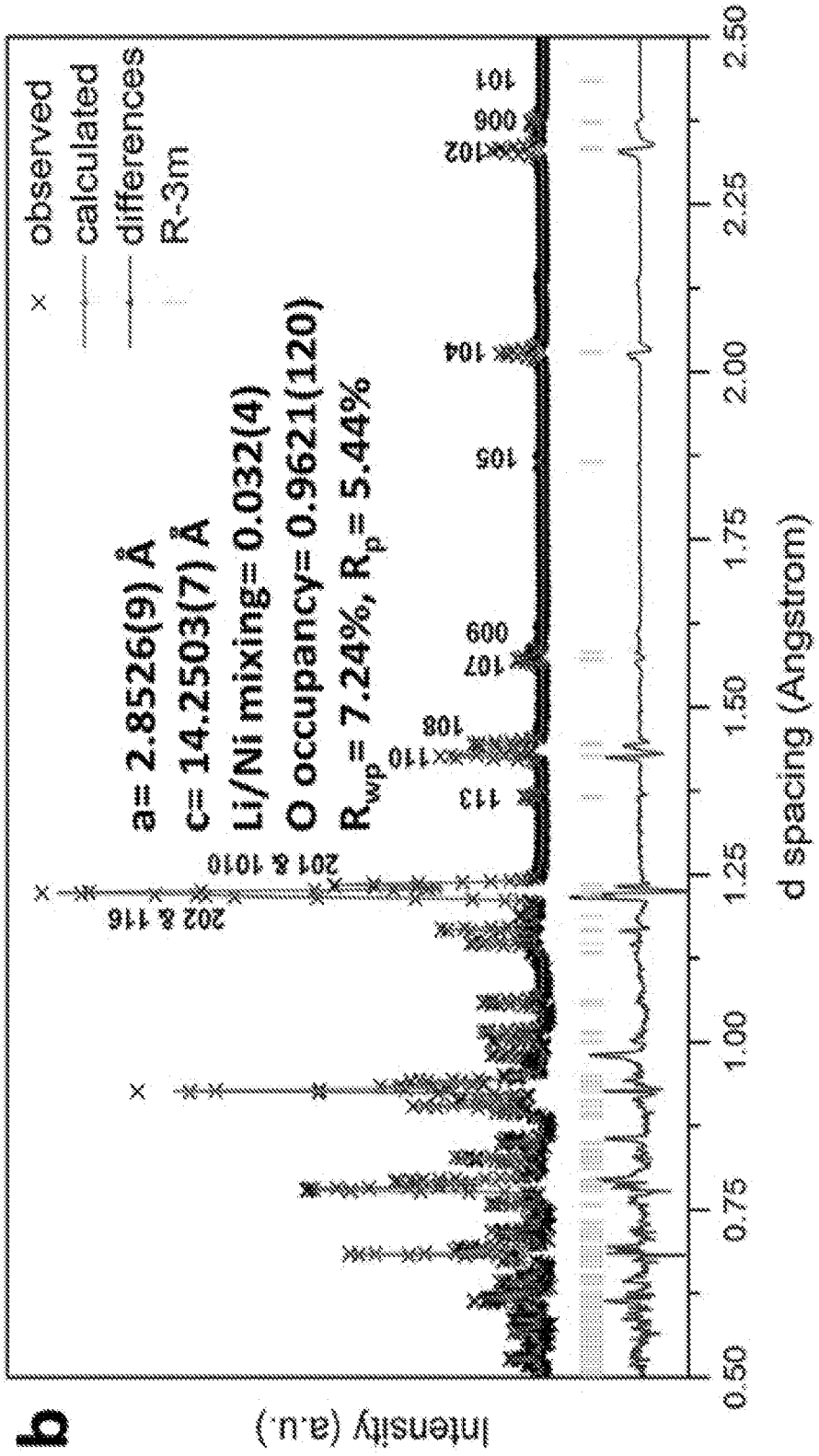
b
Intensity (a.u.)
d spacing (Angstrom)
0.50
0.75
1.00
1.25
1.50
1.75
2.00
2.25
2.50
observed
calculated
differences
R-3m
a= 2.8526(9) Å
c= 14.2503(7) Å
Li/Ni mixing= 0.032(4)
O occupancy= 0.9621(120)
R_{wp}= 7.24%, R_p= 5.44%
101
006
102
104
105
107
009
108
110
113
201 & 1010
202 & 116

FIG. 12B

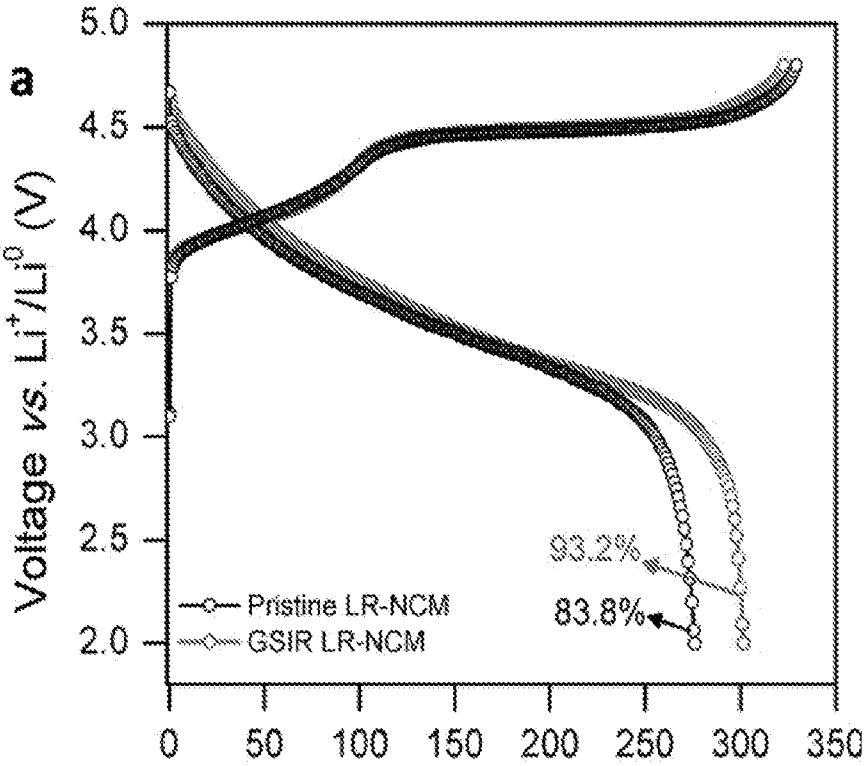

FIG. 13A

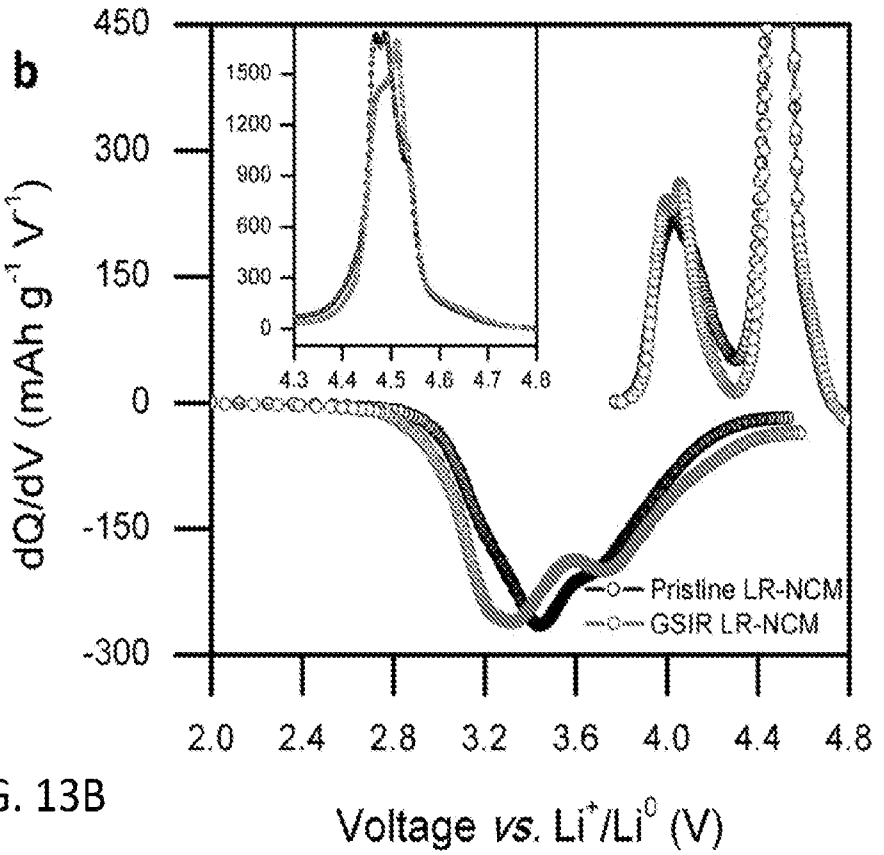

FIG. 13B

INTERNATIONAL SEARCH REPORT

International application No.
PCT/US16/62067

A. CLASSIFICATION OF SUBJECT MATTER
IPC - H01M 4/131, 4/48, 4/505, 4/525, 10/0525 (2017.01)
CPC - H01M 2/0257, 4/131, 4/48, 4/505, 4/525, 10/0525

According to International Patent Classification (IPC) or to both national classification and IPC

B. FIELDS SEARCHED

Minimum documentation searched (classification system followed by classification symbols)
See Search History document

Documentation searched other than minimum documentation to the extent that such documents are included in the fields searched
See Search History document

Electronic data base consulted during the international search (name of data base and, where practicable, search terms used)
See Search History document

C. DOCUMENTS CONSIDERED TO BE RELEVANT

Category*	Citation of document, with indication, where appropriate, of the relevant passages	Relevant to claim No.
X -- Y	(PARK, S-H et al.) "Physical and electrochemical properties of spherical Li1+x(Ni1/3Co1/3 Mn 1/3)1−xO2 cathode materials." Journal of Power Sources. 2008, Vol. 177, No. 1, abstract; figures 1, 3; pages 178, 182.	1, 13-14 ---------- 2, 3/1-2, 4/1-2, 5/1-2, 6/1-2, 7/1-2, 8/1-2, 15-20
Y	WO 2015/035712 A1 (NINGBO INSTITUTE OF MATERIALS TECHNOLOGY AND ENGINEERING, CHINESE ACADEMY OF SCIENCES) 19 March 2015; see English translation; abstract; page 3; example 14; claims 3, 6	2, 3/2, 4/2, 5/2, 6/2, 7/2, 8/2, 17-20
Y	US 8,932,768 B2 (UCHICAGO ARGONNE LLC) 13 January 2015; column 2, lines 12-17; claim 1	3/1-2, 4/1-2, 5/1-2, 6/1-2, 7/1-2, 8/1-2, 15
Y	(QIAN, D et al.) "Lithium lanthanum titanium oxides: a fast ionic conductive coating for lithium-ion battery cathodes." Chemistry of Materials. 2012, Vol. 24, No. 14, abstract; page 2744.	16
A	US 6,241,959 B1 (CHO, J-P et al.) 05 June 2001; entire document	1-2, 3/1-2, 4/1-2, 5/1-2, 6/1-2, 7/1-2, 8/1-2, 13-20
A	US 6,660,432 B2 (PAULSEN, JM et al.) 09 December 2003; entire document	1-2, 3/1-2, 4/1-2, 5/1-2, 6/1-2, 7/1-2, 8/1-2, 13-20

☐ Further documents are listed in the continuation of Box C. ☐ See patent family annex.

* Special categories of cited documents:
"A" document defining the general state of the art which is not considered to be of particular relevance
"E" earlier application or patent but published on or after the international filing date
"L" document which may throw doubts on priority claim(s) or which is cited to establish the publication date of another citation or other special reason (as specified)
"O" document referring to an oral disclosure, use, exhibition or other means
"P" document published prior to the international filing date but later than the priority date claimed
"T" later document published after the international filing date or priority date and not in conflict with the application but cited to understand the principle or theory underlying the invention
"X" document of particular relevance; the claimed invention cannot be considered novel or cannot be considered to involve an inventive step when the document is taken alone
"Y" document of particular relevance; the claimed invention cannot be considered to involve an inventive step when the document is combined with one or more other such documents, such combination being obvious to a person skilled in the art
"&" document member of the same patent family

Date of the actual completion of the international search	Date of mailing of the international search report
11 January 2017 (11.01.2017)	03 FEB 2017
Name and mailing address of the ISA/ Mail Stop PCT, Attn: ISA/US, Commissioner for Patents P.O. Box 1450, Alexandria, Virginia 22313-1450 Facsimile No. 571-273-8300	Authorized officer Shane Thomas PCT Helpdesk: 571-272-4300 PCT OSP: 571-272-7774

Form PCT/ISA/210 (second sheet) (January 2015)

INTERNATIONAL SEARCH REPORT

International application No.
PCT/US16/62067

Box No. II Observations where certain claims were found unsearchable (Continuation of item 2 of first sheet)

This international search report has not been established in respect of certain claims under Article 17(2)(a) for the following reasons:

1. ☐ Claims Nos.:
because they relate to subject matter not required to be searched by this Authority, namely:

2. ☐ Claims Nos.:
because they relate to parts of the international application that do not comply with the prescribed requirements to such an extent that no meaningful international search can be carried out, specifically:

3. ☒ Claims Nos.: 9-12
because they are dependent claims and are not drafted in accordance with the second and third sentences of Rule 6.4(a).

Box No. III Observations where unity of invention is lacking (Continuation of item 3 of first sheet)

This International Searching Authority found multiple inventions in this international application, as follows:

1. ☐ As all required additional search fees were timely paid by the applicant, this international search report covers all searchable claims.

2. ☐ As all searchable claims could be searched without effort justifying additional fees, this Authority did not invite payment of additional fees.

3. ☐ As only some of the required additional search fees were timely paid by the applicant, this international search report covers only those claims for which fees were paid, specifically claims Nos.:

4. ☐ No required additional search fees were timely paid by the applicant. Consequently, this international search report is restricted to the invention first mentioned in the claims; it is covered by claims Nos.:

Remark on Protest

☐ The additional search fees were accompanied by the applicant's protest and, where applicable, the payment of a protest fee.

☐ The additional search fees were accompanied by the applicant's protest but the applicable protest fee was not paid within the time limit specified in the invitation.

☐ No protest accompanied the payment of additional search fees.